DESIGN OF NEURAL NETWORK BASED PREDICTIVE CONTROLLER FOR PCM THERMAL

ENERGY STORAGE

By

MR. Chanachai PHUMCHA-EM

A Thesis Submitted in Partial Fulfillment of the Requirements

for Master of Engineering (CHEMICAL ENGINEERING)

Department of CHEMICAL ENGINEERING

Graduate School, Silpakorn University

Academic Year 2020

Copyright of Graduate School, Silpakorn University

การออกแบบตัวควบคุมแบบทำนายผลด้วยระบบโครงข่ายประสาทเทียมสำหรับการเก็บ
รักษาพลังงานความร้อนด้วยวัสดุเปลี่ยนสถานะ

โดย
นายชนะชัย พุ่มชะเอม

วิทยานิพนธ์นี้เป็นส่วนหนึ่งของการศึกษาตามหลักสูตรวิศวกรรมศาสตรมหาบัณฑิต
สาขาวิชาวิศวกรรมเคมี แผน ก แบบ ก 2 ระดับปริญญามหาบัณฑิต
ภาควิชาวิศวกรรมเคมี
บัณฑิตวิทยาลัย มหาวิทยาลัยศิลปากร
ปีการศึกษา 2563

DESIGN OF NEURAL NETWORK BASED PREDICTIVE CONTROLLER FOR PCM
THERMAL ENERGY STORAGE

By

MR. Chanachai PHUMCHA-EM

A Thesis Submitted in Partial Fulfillment of the Requirements
for Master of Engineering (CHEMICAL ENGINEERING)
Department of CHEMICAL ENGINEERING
Graduate School, Silpakorn University
Academic Year 2020
Copyright of Graduate School, Silpakorn University

Title	Design of Neural Network based Predictive Controller for PCM thermal energy storage
By	Chanachai PHUMCHA-EM
Field of Study	(CHEMICAL ENGINEERING)
Advisor	Assistant Professor Veerayut Lersbamrungsuk , D.Eng.

Graduate School Silpakorn University in Partial Fulfillment of the Requirements for the Master of Engineering

.... Dean of graduate school
(Associate Professor Jurairat Nunthanid, Ph.D.)

Approved by

.... Chair person
(Assistant Professor Tarawipa Puangpetch , Ph.D.)

.... Advisor
(Assistant Professor Veerayut Lersbamrungsuk , D.Eng.)

.... Committee
(Associate Professor Prakorn Ramakul , D.Eng.)

.... External Examiner
(Assistant Professor Pornsiri Kaewpradit , D.Eng.)
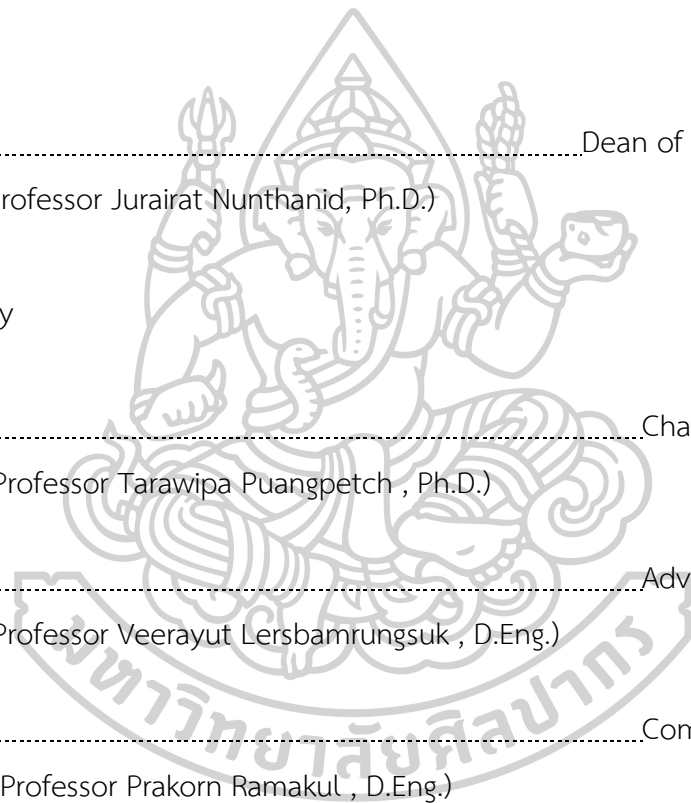
61404204 : Major (CHEMICAL ENGINEERING)

Keyword : Artificial neural network, Neural network based model predictive control, Phase change material, Thermal energy storage

MR. CHANACHAI PHUMCHA-EM : DESIGN OF NEURAL NETWORK BASED PREDICTIVE CONTROLLER FOR PCM THERMAL ENERGY STORAGE THESIS ADVISOR : ASSISTANT PROFESSOR VEERAYUT LERSBAMRUNGSUK, D.Eng.
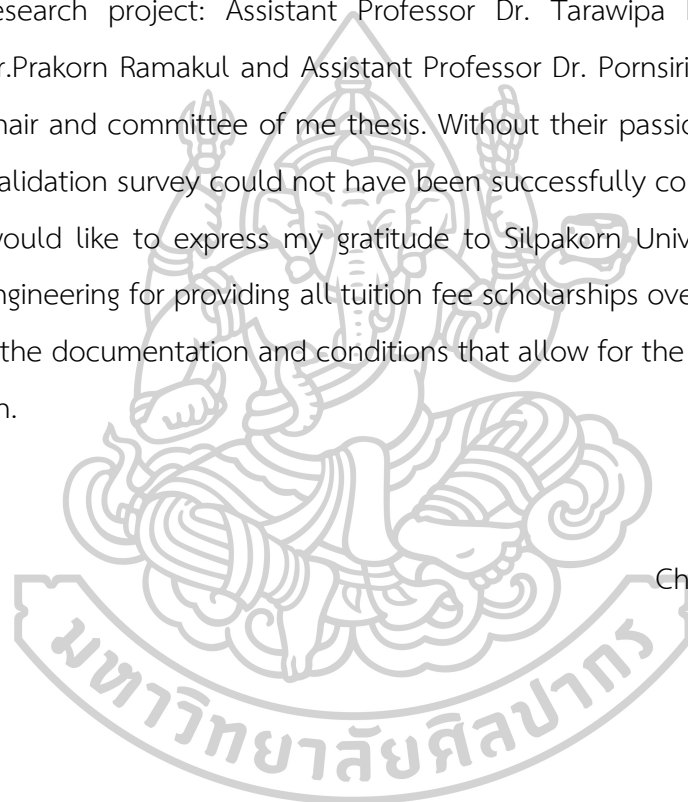
Phase change material (PCM) is a promising alternative for thermal energy storage. Due to its latent heat storage nature, large amount of heat can be stored with less change of temperature comparing with sensible heat storage. There are many applications of PCM as solar heat storage unit. In application of solar water heating, water as heat transfer fluid (HTF) is used to collect energy from sunlight during daytime. In case excess energy is available, it will be stored or charged to PCM, and released or discharged for use during night-time. In PCM charging process, there is usually no need of temperature control. However, in PCM discharging process, target temperature of hot water for indoor use is required. The objectives of this research are development of ANN model for the PCM discharging process, and design of temperature control of hot water in PCM discharging process for indoor use. In development of ANN model, two approaches were proposed. The first approach was to use feedforward neural network directly to predict PCM behavior. Inputs of the ANN includes time, HTF inlet temperature, mass flowrate, and initial PCM temperature. In the second approach, feedforward neural network was used to predict parameters of nonlinear autoregressive exogenous (NARX) model which was used to predict PCM behavior. In design of temperature control of hot water in PCM discharging process, a bypass was additionally installed and used as manipulated variable. PI and MPC controllers were designed. Although both controllers could control the temperature, MPC provided better control performance.

ACKNOWLEDGEMENTS

TABLE OF CONTENTS

LIST OF TABLES

LIST OF FIGURES

CHAPTER I

INTRODUCTION

1.1   Motivation

The beneficial aspect of thermal energy storage technology is an important way in conserving accessible energy and improving its utilization for a decade. The phase change materials (PCMs), utilized as latent heat storage units (LHSU), are promising candidates for heat storage mediums. The PCMs are becoming important thermal energy storage because of their ability to store large amount of energy. Recently, PMC based LHSU have gained considerable attention in many applications such as waste heat recovery [1, 2] solar water heating system [3-6], energy storage in buildings [7, 8],etc.

In solar thermal collectors, where heat transfer fluid (HTF) is used to collect solar energy from sunlight, PCMs can be used to store excess energy at day time and release it to HTF at night. In discharging of energy to HTF, temperature control of HTF is needed to ensure the requirement of use (such as water heater, or steam generation). However, phase change of PCMs during thermal charging/discharging can alter values of thermal properties (e.g., heat capacity, thermal conductivity, etc.) and this makes temperature control of HTF a challenging task.

In this work, packed bed PCM is one of the many types of PCMs commonly used in heating storage [9-12]. As stated previously, temperature control of HTF is needed, hence, model predictive control (MPC) will be designed for this purpose. MPC is widely used in industries and a large number of implementation algorithms has been presented. MPC use process model to predict the future behavior of a plant. The most important advantage of the MPC technology comes from the process model itself which allows the controller to deal with an exact replica of the real process dynamics. Furthermore, the constraints with respect to input and output signals are considered in the control calculation, resulting in very rare or even no constraint violation. The addition of the constraints is the feature that most clearly decides MPC from other process control techniques, leading to a tighter control and a more reliable controller.

To design of temperature control system, it is needed to understand dynamic behavior of the PCM system. Although dynamic models of PCM system have been proposed in literatures[13], the resulting models are quite complex and not able to be used in design of model-based controller (e.g., model predictive controller). This motivates a need of simplified input/output models using artificial neural network (ANN)

Artificial neural network (ANN) is non-linear systems whose structures are based on principles stimulated by the biological nervous systems of humans. An ANN consists of a large number of simple processors linked by weighted connections. By analogy, the processing units are called neurons. This technique has been applied in many disciplines of science and has produced primary results in many areas of modeling system.

In this research, ANN model for PCM packed bed heat storage unit will be developed. The model of Shuangmao will be simulated and used for generation of datasets for ANN training. After that the proposed ANN model will be incorporated into model predictive controller (MPC) where the MPC will be designed for temperature control of HTF during discharging stage of the PCM system.

1.2 Objective
- Develop artificial neural network (ANN) model for PCM based thermal energy storage

- Design of neural network-based model predictive controller for PCM based thermal energy storage

1.3 Scope of research
- Simulate packed bed thermal energy storage of PCMs and generate a number of data for ANN training datasets where input data are time, inlet HTF temperature, mass flowrate and PCM initial temperature. An output data is outlet HTF temperature.
- Develop ANN model for packed bed thermal energy storage that are applicable for prediction of the system behavior.

- Develop ANN model for packed bed thermal energy storage that is suitable for MPC controller.

- Design PI control for packed bed thermal energy storage.

- Design neural network predictive control for packed bed thermal energy storage.

1.4 Contribution of Research

- ANN models of PCM packed bed thermal energy storage.

- Neural network predictive controller for PCM packed bed thermal energy storage.
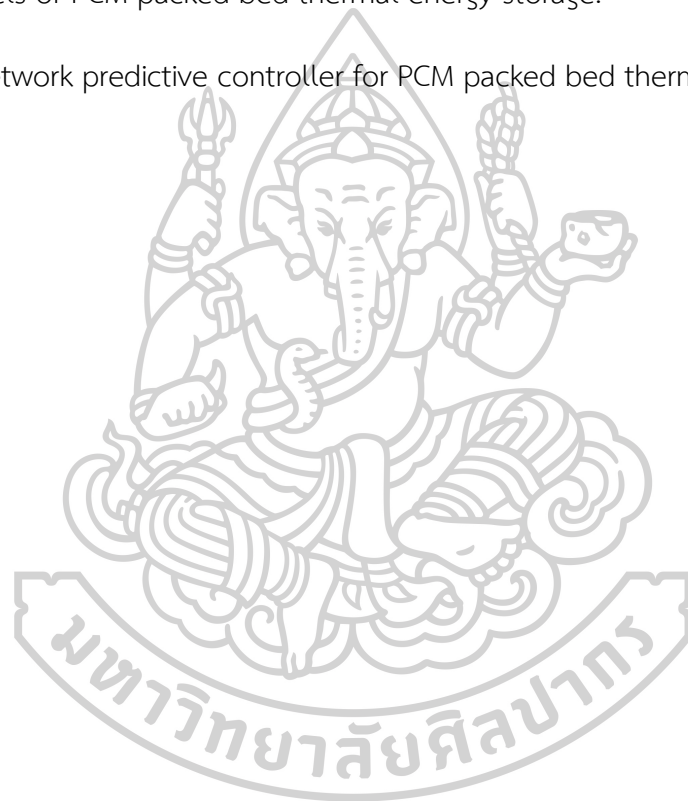
1.5 Definitions

Parameters	Definitions
A_c	Cross area of the cylindrical tank
a_p	surface area of PCM capsules per volume ($\mathbf{m^{-1}}$)
a_w	convective wall area of packed bed tank per volume ($\mathbf{m^{-1}}$)
c_f	specific heat of HTF ($\mathbf{kJ\ kg^{-1}K^{-1}}$)
c_l	specific heat of liquid phase PCM ($\mathbf{kJ\ kg^{-1}K^{-1}}$)
c_s	specific heat of solid phase PCM ($\mathbf{kJ\ kg^{-1}K^{-1}}$)
h	Coefficient convective heat transfer
h_{eff}	effective coefficient of convective heat transfer ($\mathbf{W\ m^2K^{-1}}$)
h_w	convective coefficient of heat transfer between packed bed and ambient ($\mathbf{W\ m^2K^{-1}}$)
k_f	thermal conductivity of HTF ($\mathbf{W\ m^{-1}K^{-1}}$)
k_l	thermal conductivity of liquid phase PCM ($\mathbf{W\ m^{-1}K^{-1}}$)
k_s	thermal conductivity of solid phase PCM ($\mathbf{W\ m^{-1}K^{-1}}$)
L	solidification latent heat of PCM ($\mathbf{kJ\ kg^{-1}}$)
q_{total}	total flow rate of HTF ($\mathbf{kg\ m^{-1}}$)
q_1	mass flow rate through packed bed ($\mathbf{kg\ m^{-1}}$)
q_2	mass flow rate through mixer ($\mathbf{kg\ m^{-1}}$)
T_f	temperature of HTF ($\mathbf{C°}$)
T_s	solidification temperature of PCM ($\mathbf{C°}$)
T_i	initial HTF temperature ($\mathbf{C°}$)
T_{in}	inlet temperature of HTF ($\mathbf{C°}$)
T_P	temperature of PCM ($\mathbf{C°}$)
T_{sur}	temperature of surroundings ($\mathbf{C°}$)

Parameters	Definitions
t	time ($\mathbf{s}$)
u	the velocity of the fluid flow ($\mathbf{m\ s^{-1}}$)
x	location of the flow direction ($\mathbf{m}$)
ρ_f	density of HTF ($\mathbf{kg\ m^{-3}}$)
ρ_l	density of liquid phase PCM ($\mathbf{kg\ m^{-3}}$)
ρ_s	density of solid phase PCM ($\mathbf{kg\ m^{-3}}$)
ε	void fraction of packed bed
$\emptyset$	the solid fraction of PCM
P_s	splitter percent size
t	time ($\mathbf{s}$)
Nu	Nusselt number
Pr	Prandtl number
Re	Reynold number
M_s	The ratio of the thermal resistance of solidified PCM
M_c	the cover of capsules to the thermal resistance
Nu	Nusselt number
Pr	Prandtl number
Re	Reynold number
M_s	The ratio of the thermal resistance of solidified PCM
r_i	inner radius of capsule (m)
r_o	outer radius of capsule (m)
r_p	solid-liquid interface (m)

CHAPTER II
LITERATURE REVIEWS

2.1 Overview

Energy storage can be accomplished using a variety of technologies. Various methods for capturing and harvesting energy are used depending on the type of energy stored. Energy can be stored in a variety of ways, including magnetic, mechanical, chemical, and thermal. Thermal energy storage is investigated for the purposes of this study. The mechanisms used in each category divide the methods for storing thermal energy into three categories. Sensible heat storage is the oldest and most widely used mechanism. During the charging or discharging process, sensible heat storage systems make use of the heat capacity and temperature change of the storing material. The temperature of the storage material rises when energy is absorbed during the charging process and falls when energy is released during the discharging phase. Phase Change Materials are the materials used as storage mediums in Latent Heat storage mechanisms. PCMs are substances that release or absorb energy as they transition from one phase to the next. Solid to liquid and solid to solid phase transitions are the most commonly used for heating, cooling, and domestic hot water (DHW) applications, whereas solid to gas and liquid to gas transitions have high energy transfer but are rarely used due to the large volume change during phase change.

Heat transfer in phase change materials (PCMs) during melting and solidification is a highly nonlinear phenomenon that can only be solved analytically in very simple situations. The most common solution to the phase change problem is to use finite difference methods, which discretize both space and time. The timestep and space discretization size are directly related to the accuracy of these methods. Short timesteps and small space discretization are required to obtain accurate results, implying high computational costs.

Artificial Neural Networks (ANN) appear to be a viable alternative for dealing with this issue. ANNs are artificial neurons that mimic the behavior of biological neurons. Neurons are highly interconnected cells that perform simple tasks individually but can solve complex problems when connected together[14]. Artificial neurons follow this pattern and are made up of simple mathematical functions that are linked to other similar neurons. The neurons' outputs are used as inputs for neurons in the next layer, resulting in a powerful parallel computing scheme. ANNs can deal with non-linear problems, learn from examples, are fault tolerant, can handle noisy and incomplete data, and can solve problems quickly once trained [15].

2.2 Phase change materials and application

Phase change materials are the thermal energy storage materials used in LHS systems (PCM). A wide variety of phase change materials with a wide range of melting points have been identified and thoroughly investigated. Organics (paraffins and fatty acids), inorganics (salt hydrates and metallic), and eutectic combinations of organic and inorganic materials are among the PCMs. Figure 1 shows a detailed classification of PCM for latent heat storage applications.
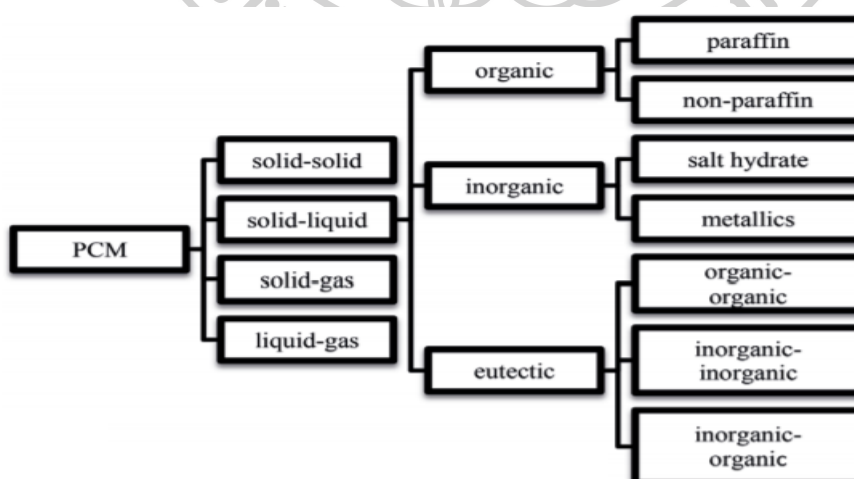
Figure 1 Classification of PCMs [16].

The selection of the PCM, which plays an important role in the development of the latent heat storage unit (LHSU), has a significant impact on the LHSU's success. The feasibility of using a specific PCM for an LHSU is determined by some of the PCM's desirable thermophysical, kinetic, and chemical properties. Table 1 lists the desirable thermal, physical, kinetic, chemical, and economic properties of PCM. Because no single material can possess all of the properties required for an ideal thermal storage medium, one must make do with what is available and attempt to compensate for the lack of physical properties through system design. As a result, researchers face a challenge in selecting appropriate PCM.

Table 1 Desired properties of PCM[16, 17]

Kinetic properties:	- When freezing, use little or no supercooling (supercooling of more than a few degrees interferes with proper heat extraction). - Extremely high nucleation and crystal growth rates. The melt should crystallize at its thermodynamic freezing point, in other words. - Efficient heat transfer, particularly at isothermal temperatures.
Chemical properties:	- Non-corrosiveness to the construction material - No chemical decomposition after multiple freeze/melt cycles - There is no toxicity. - Non-explosive, non-poisonous, non-flammable, non-polluting
Physical properties:	- Low volume change during phase transition - Low volume change during phase transition - Favorable phase equilibrium - High density for smaller container volume - Low vapor pressure to reduce the problem of containment - Consistency in the congruent throughout the entire thermal cycle
Thermal properties:	- High latent heat of fusion per unit volume for better heat transfer - High thermal conductivity of solid and liquid phases for better heat transfer - Increased specific heat for more sensible heat storage
Economic criteria:	- Sufficient supply - Low cost - Ease of recycling and treatment

PCM's application Shell-tube heat exchangers, flat plates, evacuated tubes, packed beds, and other devices can all benefit from it. In the next section, we'll go over the previous research. A heat storage system with PCM spherical capsules in a packed bed configuration was numerically studied by Yang et al.[18]. Natural convection was modeled using effective conductivity, and phase change was modeled using the apparent heat capacity method, which assumes a large heat capacity in the phase change region. An in-house code described the numerical model, and the tridiagonal matrix algorithm was used to solve the discretized equations. The capsules are connected to a flat plate solar collector in series, according to the PCM freezing temperature. The chosen HTF is heated in the collector before being transferred to the packed bed configuration. The finite differences method was used to model and calculate the heat transfer mechanisms between the HTF and the capsules. The energy and exergy efficiencies of different PCMs in a packed bed configuration were compared, and it was discovered that the multiple-type packed bed melts before the single-type, and the temperature is also higher. The collector efficiency of the multiple type is also higher. The tested methods for raising the performance of a solar-PCM apparatus are shown in Fig. 2.
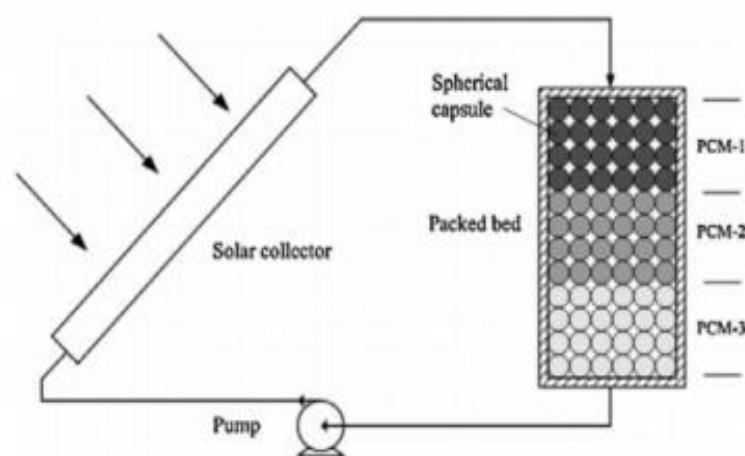
Figure 2. The tested methods for raising the performance of a solar-PCM apparatus.

Deng et al. [19] tested the performance of a prototype tank and an improved version of it, both of which had a sodium stearic trihydrate PCM layer, in the hot water tank of a solar DHW and auxiliary heating system. As shown in Fig. 3, the water volume was 148 l and the PCM mass was 35 kg, positioned around the tank between the water and the insulation. One spiral Heat exchanger (HE) was used for solar charging and the other for charging an electric heater. The solar HE must be about 10 m long, and the electric heater HE must be about 20 m long, according to the results. The PCM's heat content was lower than expected, and its properties remained stable over the course of a three-month test. Lastly,
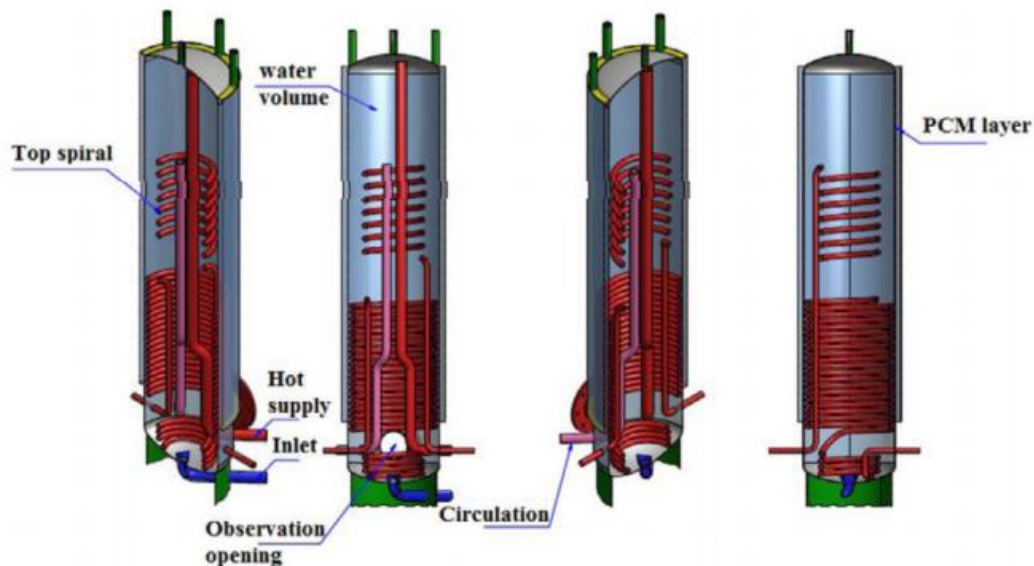
Figure 3 A 1.8 m tall water storage tank with a layer of PCM around it for DHW supply [19].

The addition of PCM to solar DHW systems is a topic of ongoing research, which can be done either in the collector itself (integrated solar collector) or separately from the collector (non-integrated). The two types of PCM addition in solar collector systems are shown in Fig. 4.
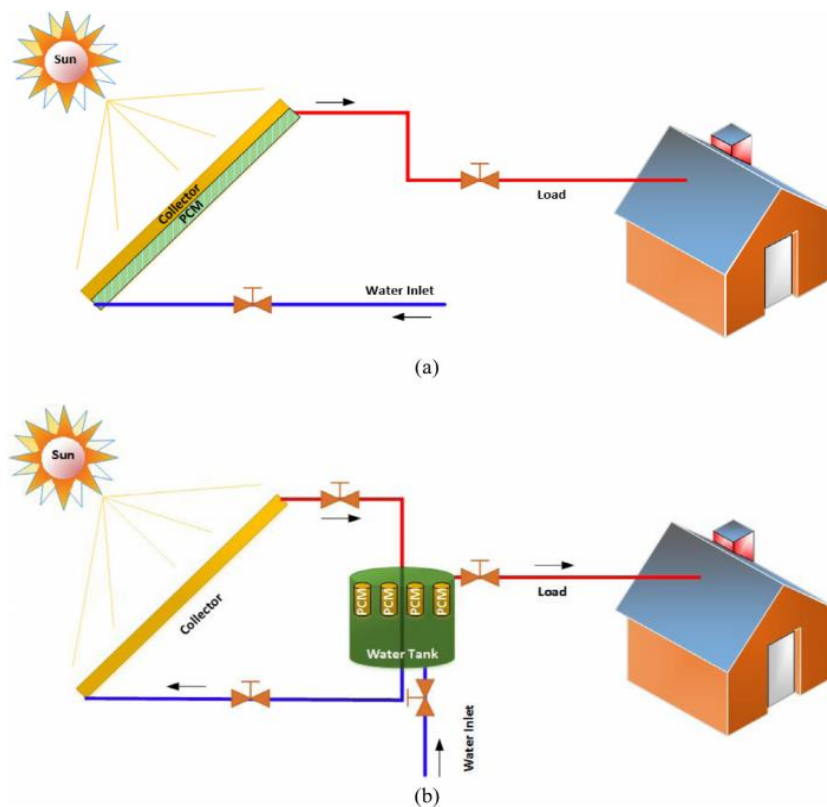
Figure 4 Solar DHW systems combined with PCM: (a) Integrated and (b) Non-Integrated

2.3 Solar thermal energy storage with PCM modelling

Thermal energy storage (TES) has been highlighted as a technology that may assist in the management and control of these systems by resolving this mismatch or by using peak load shifting techniques Latent thermal energy storage systems have been widely explored and are regarded to be more energy dense, efficient, and compact [20, 21]. In this context, packed bed latent heat storage systems have garnered considerable attention due to the large area of contact between the storage (spheres of phase change material) and the heat transmission fluid (HTF). These packed bed TES systems have been applied to a variety of applications, including solar thermal energy storage [22], compressed air energy storage [23], solar cooling, combined heat and power plants (CPW), low temperature storage systems for central air conditioning,

energy efficient buildings, and waste heat recovery systems . Optimization of the design and control of such TES systems is required to overcome the technology's technical and economic constraints. Numerous experimental studies have been conducted in this area to determine the system's thermal properties during freezing and melting processes. Cho and Choi [24][conducted a parametric study based on Reynolds number and inlet temperature to compare the performance of paraffin in a packed bed system to that of a system using water as the storage material. They concluded that the average heat transfer coefficient for paraffin was up to 40% greater than that of water during both freezing and melting; additionally, they observed that the average heat transfer coefficient for paraffin was up to 40% greater than that of water. Nallusamy et al. [25] also used paraffin in a packed bed system to investigate the effect of porosity and HTF flow rate on the system's performance. The authors concluded that the use of packed bed phase change materials (PCM) results in a smaller storage tank when compared to conventional sensible storage tanks. Oró et al. [26] also explored stratification inside the tank experimentally, indicating that the use of a latent heat storage packed bed promotes stratification during the discharge process.

Despite the experimental results, the complicated transient nature of the latent packed bed TES system, as well as the expensive cost of the setups, necessitates the use of numerical 3 models to further investigate the system's performance. Numerous models for numerically forecasting the thermal performance of a packed bed Latent Thermal Energy Storage (LTES) system (Figure 5) based on a cylindrical tank filled with spheres containing PCM have been developed.
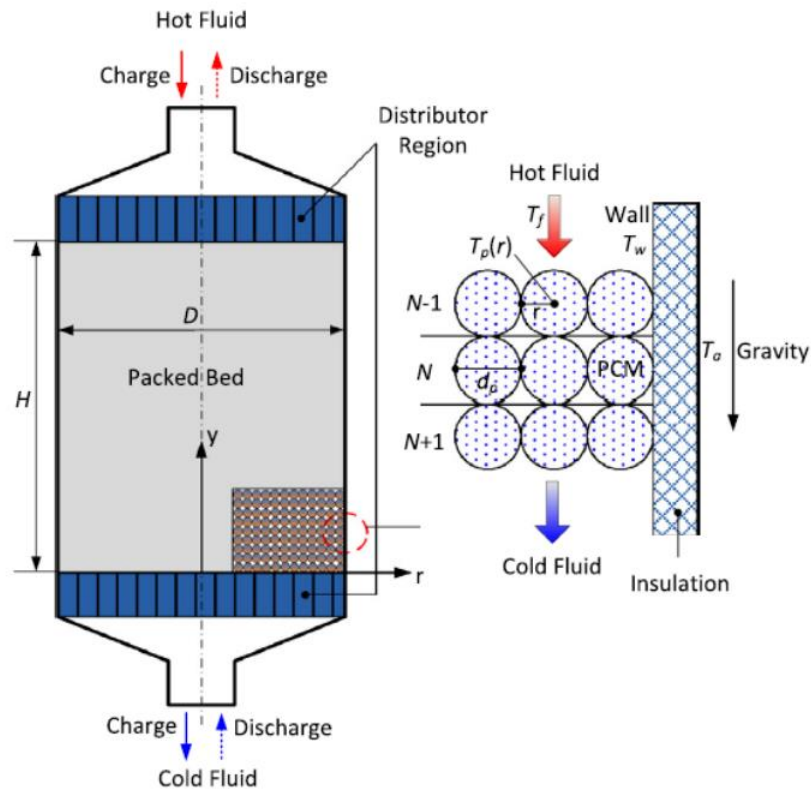
Figure 5 Sketch of a packed bed thermal storage system [27]

Single phase models

The fluid and solid phases were regarded as a single element in single phase models, hence both phases were discretized. The following is an example of an energy equation:

$$\varepsilon \cdot C_{P,f} \cdot \rho_{HTF} \cdot \frac{\partial T}{\partial t} + (1-\varepsilon) \rho_{PCM} \frac{\partial H}{\partial t} + C_{P,f} \cdot \rho_f \cdot u \cdot \frac{\partial T}{\partial y} = k_{eff,y} \frac{\partial^2 T}{\partial y^2} + k_{eff,r} \left(\frac{\partial^2 T}{\partial r^2} + \frac{\partial T}{2 \cdot \partial r} \right) \quad (2.1)$$

The accumulative term of the heat transfer fluid and the PCM are the first two terms of the formula, respectively. The HTF's convective term is represented by the final term on the left, while the two terms on the right represent conduction in the axial and radial directions, respectively. In the border nodes, heat losses to the environment may be included.

The assumption that the HTF and PCM are at the same instantaneous temperature is only true when utilizing solid particles with extremely high thermal 6 conductivity, hence this technique is not often used for characterizing PCM packed bed systems. The restricted thermal conductivity of the PCM is well known, with paraffin and fatty acids having approximately 0.2 W/m.K and salts hydrate having roughly 0.6 W/m.K [28].

Schumann's model[29]:

This two-phase model is based on one-dimensional heat transfer and ignores heat conduction in both the fluid and solid phases. The energy conservation equations are stated separately for the HTF and the solid particles, as in all two-phase models, and must be solved concurrently.

Heat transfer fluid:

$$\varepsilon \cdot C_{P,f} \cdot \rho_f \left(\frac{\partial T_f}{\partial t} + u \frac{\partial T_f}{\partial y} \right) = h_{PCM-HTF} \left(T_{PCM} - T_f \right) - U_L \left(T_f - T_{ENV} \right) \tag{2.2}$$

Phase change material:

$$(1-\varepsilon) \rho_{PCM} \cdot \frac{\partial H}{\partial t} = h_{PCM-HTF} \left(T_f - T_{PCM} \right) \tag{2.3}$$

The primary limitation of Schumann's model is that it does not account for thermal diffusion within solid particles; as a result, no thermal gradients are considered in the spheres, and heat conduction is not taken into account in the model because only convection is used to drive the heat transfer process. However, as previously mentioned, PCMs have a poor thermal conductivity, which means that heat conduction thermal resistance plays a crucial role in heat transmission during both charge and discharge operations. As a result, some writers have modified Schumann's model to account for conductive thermal resistance by included the sphere's conductive thermal resistance in the convective heat transfer at the solid-fluid

interface. Regin et al. [30] utilized a modified version of Schumann's model to investigate the behavior of a packed bed latent heat thermal energy storage system utilized in a solar water heating system. Using an outer surface overall heat transfer coefficient U0, the model incorporates the conductive resistive layers of the shell and solid sections of PCM into the energy equation at the solid-fluid interface. This coefficient changes depending on whether the spheres are entirely liquid, totally solid, or in the middle of a phase transition. It's also defined as follows:

$$U_0 = \frac{1}{A} \cdot \frac{1}{R_{ext} + R_c + R_{in}(t)} \tag{2.4}$$

Concentric dispersion model:

The packed bed is treated as an isotropic porous medium consisting of independent spherical particles in this technique, which is based on a two-phase model. This is the sole method for resolving the temperature distribution inside solid particles. Axial heat conduction in the heat transfer fluid and/or the PCM are examples. As a result, the energy conservation equation is (PCM at border and PCM within the sphere, respectively):

$$\varepsilon \cdot C_{P,f} \cdot \rho_f \left(\frac{\partial T_f}{\partial t} + u \frac{\partial T_f}{\partial y} \right) = \varepsilon \cdot k_f \frac{\partial^2 T}{\partial y^2} + h_{PCM-HTF} \left(T_{PCM} - T_f \right) - U_L \left(T_f - T_{ENV} \right) \tag{2.5}$$

$$(1-\varepsilon) \rho_{PCM} \cdot \frac{\partial H}{\partial t} = (1-\varepsilon) k_{PCM} \frac{\partial^2 T}{\partial y^2} + h_{PCM-HTF} \left(T_f - T_{PCM} \right) \tag{2.6}$$

$$\rho_{PCM} \cdot \frac{\partial H}{\partial t} = \frac{1}{r^2} \cdot \frac{\partial}{\partial r} \left(k_{PCM} \cdot r^2 \cdot \frac{\partial T}{\partial r} \right) \tag{2.7}$$

The cylindrical container is split into elements in the axial direction in concentric dispersion models, and the fluid temperature is assumed to be uniform. All spheres of the same height are assumed to act equally, and just one sphere is typically discretized and solved, as illustrated in Figure6. Furthermore, heat losses to the environment may be easily included in such models.
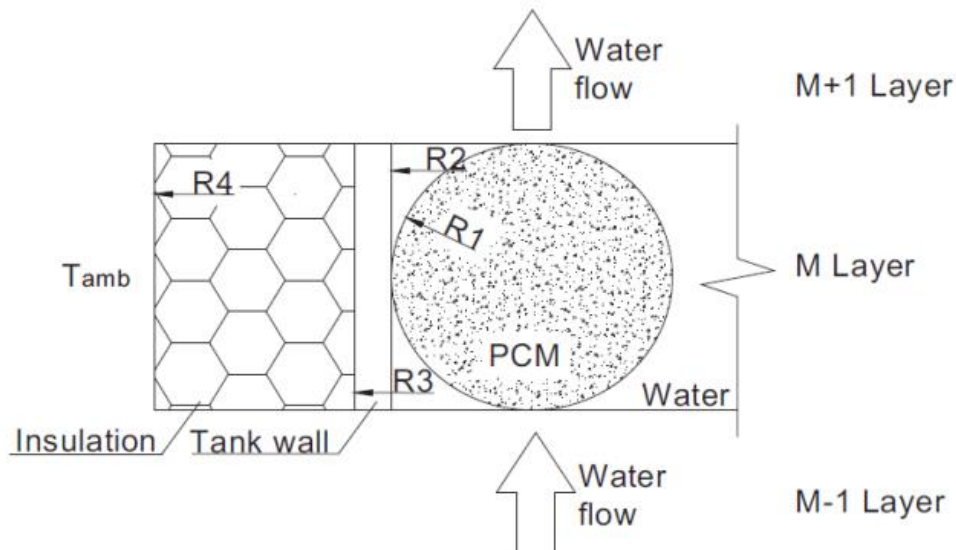
Figure 6 Sketch of discretized domain in Concentric Dispersion Method [36]

2.4 PCM thermal energy storage with artificial neural network

Al Abdallat [31] was studied performance of a thermal energy storage system with and without a phase change material was investigated using three Artificial Neural Network models (Feedforward, Elman, and Nonlinear Autoregressive Exogenous (NARX) networks). The neural network was trained using previously collected experimental data. The input layer of the network used time, mass of water, mass flow rate, number of balls containing the PCM, hourly solar radiation, ambient temperature, and inlet water temperature. The temperature of the outlet water was in the output layer. The architecture of ANN used for this study shown in Fig. 7. The obtained results were compared to experimental data previously obtained. The Elman, feedforward, and NARX models' coefficients of determination were found to be 0.95006, 0.99411, and 0.88185, respectively, indicating that the Artificial Neural Network technique could be used to estimate the outlet temperature with excellent accuracy. The results revealed that the feedforward model had the best ability to estimate the required performance, while the NARX and Elman networks had the worst.
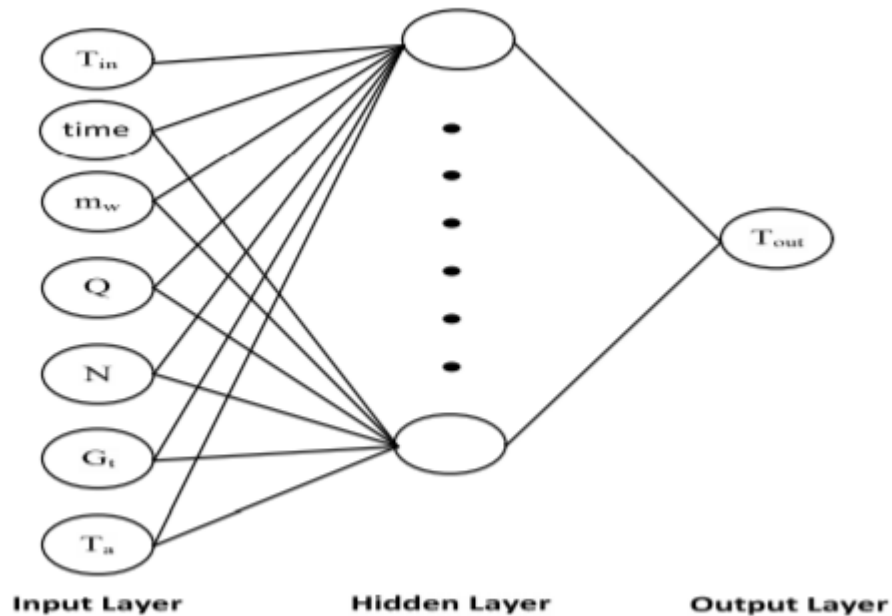
Figure 7 The architecture of ANN used for this study [31].

Ermis [32], the author applied a feed-forward back-propagation artificial neural network (ANN) algorithm for heat transfer analysis of phase change process in a latent heat thermal energy storage system. ANNs are modeled as a multi-input, it consists of heat transfer area, inlet heat transfer fluid temperature, Reynold number and time. The output of ANN model is total energy storage show in figure 8. The trained ANN model with an absolute mean relative error shows good performance to predict the total amount of heat stored compares with experimental data. In 2007, I. Taymaz and Y. Islamoglu studied the ability of an artificial neural network (ANN) model for heat transfer analysis in a converging–diverging tube using back propagation learning method, the most common method for ANNs, was used in training and testing neural network that was trained by selected values of the Reynolds numbers, Prandtl numbers, half taper angle, aspect ratio and Nusselt number. This result showed a respectable neural network model for laminar air flow in converging-diverging tube.
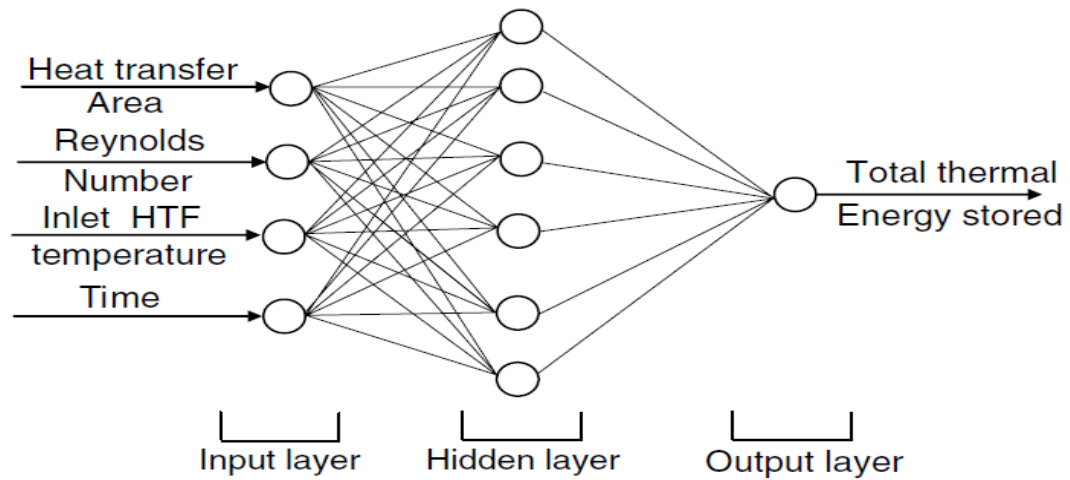
Figure 8 A three-layer feed-forward back-propagation neural network for heat transfer analysis.

Delcroix [33], The purpose of this article is to demonstrate how Artificial Neural Networks (ANNs) may be used to simulate the heat capacity of Phase-Change Materials (PCMs) using data from Differential Scanning Calorimetry (DSC) tests and experiments. Coefficients of determination of 0.99 and 0.66 are found utilizing two independent variables (DSC test) and four independent variables (experiments) to mimic the dependent variable, i.e., PCM heat capacity. The independent variables include the PCM temperature and heat transfer properties such as the rate of heating and cooling, the duration of heating and cooling, and the prior condition (temperature and heat capacity). These findings demonstrate that ANNs may be utilized to simulate PCMs when valid independent variables are included.
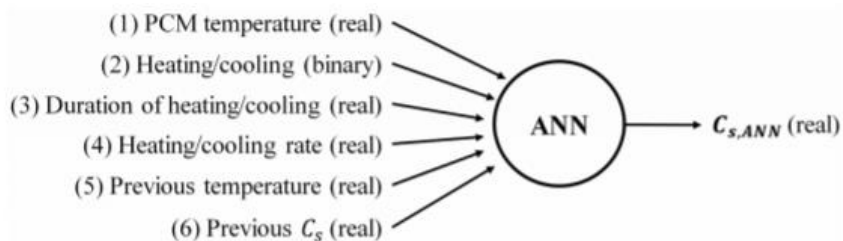
Figure 9 The procedure for generating an ANN using experimental data

Baby and Balaji [34],The time required to attain a set-point temperature is determined for aluminum finned heat sinks loaded with the phase transition material n-eicosane. To forecast operation times, the collected results are combined using a feed-forward back-propagation artificial neural network. The optimal design that optimizes thermal performance is then determined using the artificial neural network prediction. Four distinct plate-fin heat sink designs filled with phase change materials with varying aluminum volume percentages were studied experimentally.
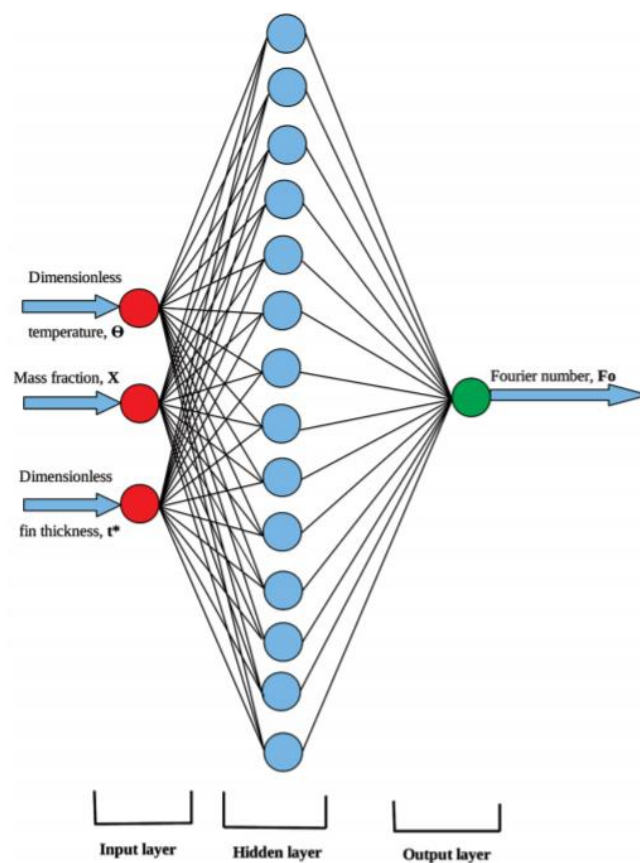
Figure 10 the neuron architecture. (a color illustration is accessible online) [34]

2.5 Neural network-based model predictive controller

Draeger, Engell, and Ranke [35] demonstrated how to manage the pH in a laboratory-scale neutralization reactor using a neural network-based model predictive control technique. They manage the pH-value using a feedforward neural network as the nonlinear prediction model in an expanded DMC method. The training algorithm is a mixture of a backpropagation method and an adaptive backpropagation method. This combination has been fine-tuned to be very resilient against being trapped in local minima and to be completely oblivious to the initial settings of the network's weights.

Lazar and Pastravanu [36], The design and implementation of a neural network-based predictive controller for governing the dynamics of non-linear processes are investigated. The benefits of utilizing neural networks to describe non-linear processes are discussed, as well as how to design neural predictors. The author demonstrated that a neural predictive controller application may eliminate the difficulties associated with non-linear predictive control applications by simplifying the building of non-linear models and providing a rapid, reliable solution to the control algorithm. The controller is designed and implemented for a plant that is commonly referred to in the literature. The results of simulation tests are presented to illustrate the efficacy of the suggested strategy.

Yu and Zhu [37] developed an intriguing way of nonlinear control using predictive controllers. The approach is based on a digital recurrent network (DRN) model of the controlled system, which is used to forecast the future behavior of the output variables, as seen in Figure 11. Where the network's output is located:

$$y_m(k) = \sum_{i=1}^{n_H} \omega_i v_i + b \tag{2.8}$$

The cost function that minimizes the difference between future object output values and intended output values is as follows:

$$J(k) = \sum_{i=1}^{N_H}[r(k+1) - y_m(k+1)]^2 + \alpha \sum_{i=1}^{N_c} \Delta u^2(k+l-1) \tag{2.9}$$

Finally, the future object outputs and their intended values are stated by. The function ga of Matlab's Genetic Algorithm Optimization Toolbox is used to determine the optimal control signal values.
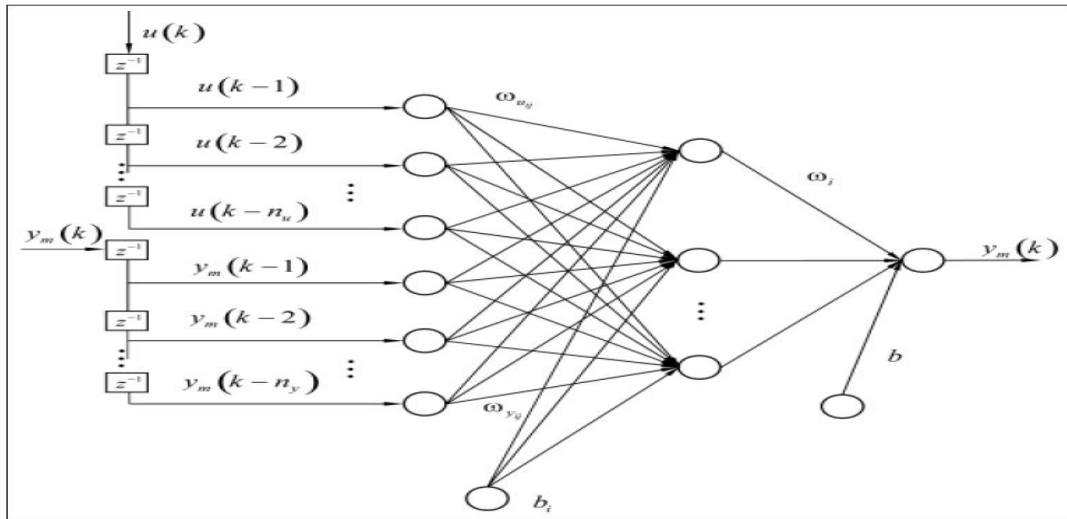
Figure 11 Digital recurrent network (DMC).

Hang, Hao, and Yu-He [38], The NARX network is a dynamical neural design that is often used to describe nonlinear dynamical systems' input-output relationships. When used for time series prediction, the NARX network is implemented as a feedforward time delay neural network (TDNN), which eliminates the feedback loop of delayed outputs, significantly lowering its predictive ability. The purpose of this research is to demonstrate how the NARX network's original design can be readily and effectively used to time series prediction by using embedding theory to rebuild the NARX network's input. We assess the suggested methodology using real-world data from a Co2 compressor. The findings demonstrate that the suggested technique outperforms established neural network-based predictors, such as the TDNN design, on a consistent basis.
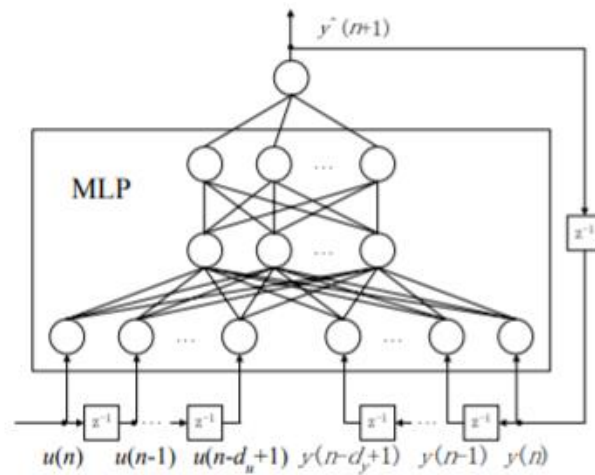
Figure 12 NARX network with du delayed inputs and dy delayed outputs (z-1 is the unit time delay).

CHAPTER III

THEORY

3.1 Solar thermal energy storage with PCM

Due to its increased heat storage capacity and more isothermal behavior during charging and discharging, latent heat storage or thermal energy storage with PCM is one of the most efficient ways for storing thermal energy. As a consequence, phase change materials are now frequently used in practice to improve the storage capacity of a variety of thermal energy systems. Latent heat storage materials are phase change materials (PCMs). The chemical bonds inside the PCM break apart when the source temperature increases, causing the material to transition from solid to liquid (as is the case for solid-liquid PCMs). Because the phase transition is an endothermic (heat-seeking) process, the PCM absorbs heat. When the phase transition temperature is achieved, the heat stored in the storage medium starts to melt. The temperature is then maintained at the same level until the melting process is completed. The heat accumulated during a material's phase shift (melting process) is referred to as latent heat. The advantages of latent heat storage are as follows: a) it is possible to store large amounts of heat with only small temperature changes, resulting in a high storage density; and b) because the change of phase at a constant temperature takes some time to complete, temperature variations can be smoothed. When comparing latent

and sensible heat storage, it can be shown that latent heat storage may achieve storage densities that are generally 5 to 10 times greater. The volume of PCM storage is two times that of water. In a broad temperature range, latent heat storage may be exploited. A vast variety of PCMs have been found to melt at any needed heat of fusion. The PCM utilized in thermal storage system design should have appropriate thermophysical, kinetics, and chemical characteristics.

3.2 Numerical optimization problem

3.2.1 Levenberg–Marquardt backpropagation algorithm

The Levenberg-Marquardt algorithm combines these two approaches and alternates between them based on the requirements and progress toward reducing the Least Mean Squares goal function defined in below.

$$[\mathbf{J}^\top \mathbf{W} \mathbf{J} + \lambda \mathbf{I}] \mathbf{h_{lm}} = \mathbf{J}^\top \mathbf{W} (\mathbf{y} - \hat{\mathbf{y}}), \qquad (3.1)$$

When a Gauss-Newton Method is used for small values of the parameter and a gradient descent update is used for big values of the same parameter. That parameter is first set to a big value, resulting in short steps in the sharpest descent direction. If one iteration's approximation causes a worse mistake, then is raised. The Levenberg-Marquardt algorithm approaches the Gauss-Newton technique, converging quicker to a local minimum of the objective function as the solution approaches [39].If any of the following circumstances are satisfied, the Matlab implementation of the LM technique will come to a halt:

1. The maximum number of epochs (iterations of training) has been achieved.

2. The time limit has been exceeded

3. The performance objective has been accomplished.

4. The performance gradient falls below a certain threshold.

5. λ exceeds λmax

6. Validation performance has improved for an extended period of time.

This strategy has shown to be quite practical, and it has become the de facto standard for optimizing medium-sized nonlinear models. It will be significantly quicker than the gradient descent approach for medium-sized networks with a few hundred parameters. However, since each iteration involves a matrix inversion, the expense of the inversion exceeds the method's benefits for bigger networks with more parameters. Despite the fact that it approximates the Hessian matrix, the cost of the inversion (O (N3), where N is the number of parameters) demands a lot of memory for large matrices [39].

3.2.2 Bayesian regulation backpropagation algorithm

The backpropagation neural network (BPNN) and Bayesian regularization learning technique are discussed in this section. A classical neural network design is modeled after the human brain's function. The neurons in the brain and their connections create an equivalence relation with the neurons in the neural network and their associated weight values (w). In a single layer network with many neurons, each element u_j of the input vector is assigned a weight w_{ij} and is linked with each neuron i. Generally, a constant scalar component termed bias b_i corresponding to each neuron is provided to boost the network's flexibility. This bias b_i is multiplied by a scalar input value (in this case 1,) and added to the weighted sum $w_{ij}u_j$ of the vector components u_j to get a net input n_i. This net input I is then given to an activation function f (alternatively referred to as a transfer function), which generates the output value a_i. A neural network, in general, consists of two or more layers. By including a hidden layer of neurons between the input and output layers, a multi-layer neural network, also known as a shallow neural network, is formed. Additionally, the addition of several hidden layers to a multi-layer neural network is referred as be a deep neural network.

Traditionally, a BPNN model, which is a kind of multi-layer neural network, consists of three levels: an input layer, one or more hidden layers, and an output layer, as seen in Figure 13. The input layer links the R-element input vector u with the input weight matrix W^1 and the first bias vector b^1 to provide an effective input n^1 for the activation function f^l, which generates an output vector a^l. The first layer's output vector a^l serves as the input to the hidden layer, where it is coupled with the hidden layer's weight matrix W^2 and bias vector b^2. Finally, the output of the hidden layer is fed into the output layer, which produces a predicted output a^3 with weight matrix W^3 and bias vector b^3. The weight matrix W^l and bias vector b^l for layer l (where = 1, 2,...,n) of a neural network with a total of l layers may be expressed as:

$$\mathbf{W}^l = \begin{bmatrix} w^l_{11} & w^l_{12} & w^l_{13} & \cdots & w^l_{1R} \\ w^l_{21} & w^l_{22} & w^l_{23} & \cdots & w^l_{2R} \\ \vdots & \vdots & \vdots & \ddots & \vdots \\ w^l_{N^l1} & w^l_{N^l2} & w^l_{N^l3} & \cdots & w^l_{N^lR} \end{bmatrix}, \qquad \mathbf{b}^l = \begin{bmatrix} b^l_1 \\ b^l_2 \\ \vdots \\ b^l_{N^l} \end{bmatrix}, \tag{3.2}$$

where N^l signifies the number of neurons in layer l and n^l signifies the effective input.

$$\mathbf{n}^l = \mathbf{W}^l \mathbf{a}^{l-1} + \mathbf{b}^l, \qquad \text{with } \mathbf{a}^0 = \mathbf{u}.$$

$$\tag{3.3}$$

The number of input (N^1) and output (N^3) neurons is proportional to the number of input and output vectors, respectively. The quantification of the weights and biases is, however, determined by the number of neurons in the hidden layer (N^2). The best network topology is indicated as $N^1 - N^2 - N^3$ by the optimum number of neurons in each layer needed for training. Backpropagation neural networks utilize a variety of activation functions, including hard limit, linear, sigmoid, log-sigmoid, and hyperbolic tangent sigmoid. In the present study, linear activation functions are used in all layers to ensure that the output equals the input, i.e. $a^l = n^l$.
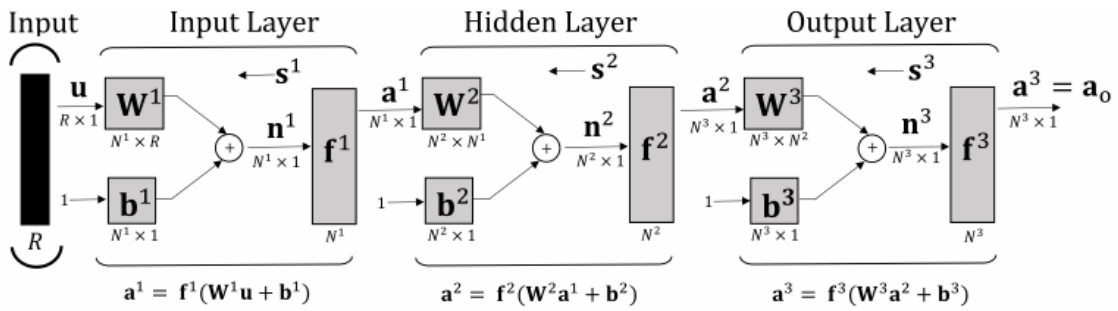
Figure 13 A characteristic backpropagation neural network with input, hidden, and output layers[40].

3.3 Artificial Neural Networks

The single-input neuron, as seen in Fig.14, is the most basic building block for neural networks. In this neuron model, there are three distinct operations that take place. The transition function, the weight function, and the biased net input function. To begin, the scalar input p is multiplied by the scalar weight w to produce the scalar product wp. Second, the net input n is formed by adding the weighted input wp to the scalar bias b. The prejudice acts as a weight by shifting the feature f to the left by a number b. Finally, the net input is fed into the transfer function f, which generates the scalar output a. The weight function, net input function, and transfer function are the names provided to these three processes. Some networks calculate the difference between them, |w-p|, rather than calculating the weight times the data. Instead of summing the bias to the weighted input, most networks use multiplication. However, the method we mentioned is the most widely known, and it is the one we would use in this project. Training should be used to change the weight w and the bias b. The teaching of a neural network is based on this foundational principle. We can get optimal behavior from the neural network by changing these parameters in order to estimate or match a complicated goal feature. Figure 15 shows the structure of a single neuron with a vector input p rather than the scalar input mentioned previously. The scale of the variable is described by R. The weight W is an R-dimensional column matrix that multiplies the input vector p in a dot product. $n = w_{1,1}p_1 + w_{1,2}p_2 + \dots + w_{1,R}p_R + b$ would be the corresponding scalar. The majority

of the systems continue to operate as they did in the single neuron model. The bias is applied to the weighted input before being sent to the output a through the desired transfer feature. The contribution of a cell with more than one neuron is a vector. This creates a layer with the weighting, bias, and transfer mechanism defined. This layer usually does not have the input layer or the vector p. The same processes occur in each layer of a multi-layered network, except that the output of the first layer is now bound to the input of the second, and the adjustable weights shape a matrix rather than a vector.

$$a = f(wp+b)$$
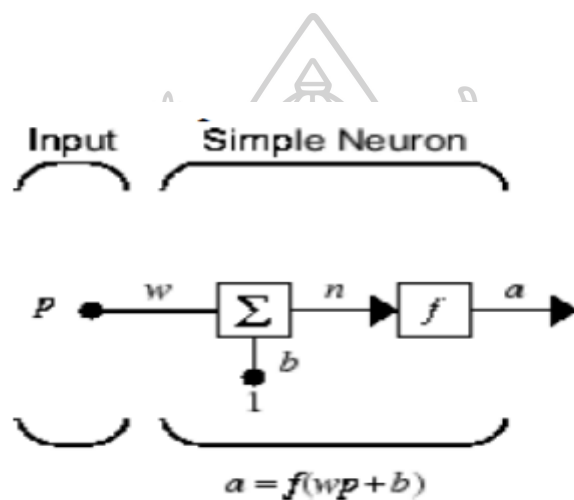
Figure 14 Single Neuron Model

$$a = f(\mathbf{W}\mathbf{p}+b)$$

Where...

R = number of elements in input vector
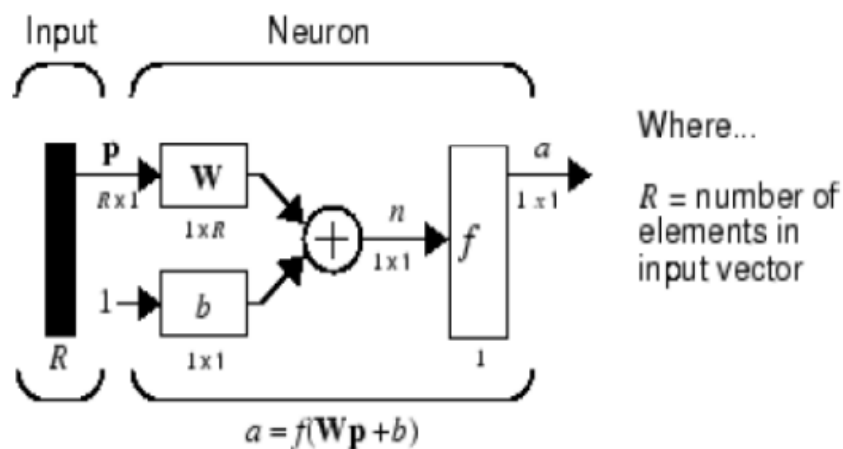
Figure 15 Layout of a single neuron with a vector input

3.3.1 Transfer function

The Linear Transfer Function shown in Fig. 16 and the Hyperbolic tangent sigmoid transfer function shown in Fig. 17 are two of the more widely used transfer functions defined and used by the Matlab program, which we use for this work. Since it is differentiable, the Log-Sigmoid transfer feature is commonly used in the inner secret layers. It compresses the inputs, which could vary from 0 to 1, to a range of 0 to 1. In the output layer, the Linear Transfer mechanism is used.

$$a = purelin(n)$$
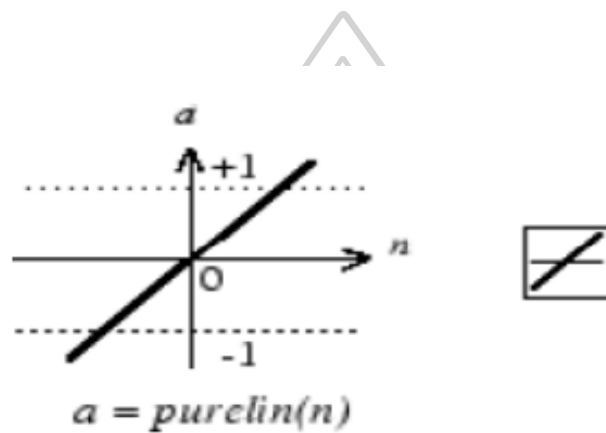
Figure 16 Linear Transfer Function
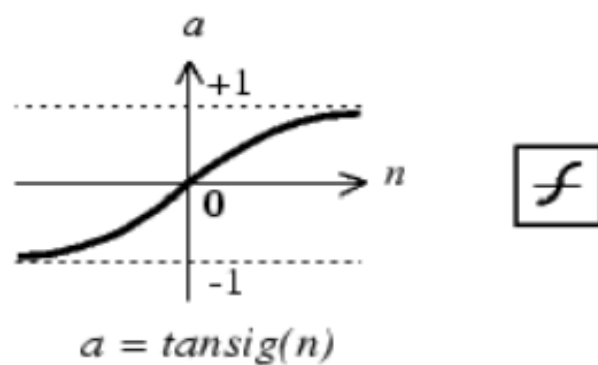
$$a = tansig(n)$$

Figure 17 Tan-Sigmoid Transfer Function

3.3.2 Feed-forward neural network

Artificial neural networks, as their name suggests, are modeled after their biological counterparts, the brain and nervous system. In terms of structure and information processing, the biological brain differs significantly from the ordinary digital computer. In many aspects, the biological brain (or, more specifically, the human brain) is significantly more powerful and superior than traditional computers. The capacity to "learn" and "adapt" is the most fundamental distinguishing attribute of a living brain, which a traditional computer lacks. Traditional computers carry out particular tasks depending on the instructions, sometimes known as "programs" or "software," that are placed into them. A "neuron" is the basic building unit of neural networks. A neuron may be thought of as a kind of processing unit. Neurons in a neural network are linked together by "synaptic weights," or "weights" for short. Each neuron in a network receives "weighted" information from the neurons to which it is connected via these synaptic connections, and produces an output by passing the weighted sum of those input signals (either external inputs from the environment or outputs from other neurons) through a "activation function." "Feed-forward neural networks" and "recurrent neural networks" are the two basic types of network topologies based on the kind of connections between the neurons. The network is referred to as a "feed-forward neural network" if there is no "feedback" from the outputs of the neurons to the inputs throughout the network. Otherwise, the network is referred to as a "recurrent neural network" if there is a synaptic link from the outputs to the inputs (either their own inputs or the inputs of other neurons). Layers are often used to organize neural networks. Feed-forward neural networks are classified as either "single layer" or "multi-layer" based on the number of layers.

3.3.3 Nonlinear Autoregressive Model with Exogenous Inputs (NARX)

The NARX (Nonlinear Autoregressive Model with Exogenous Inputs) is a kind of discrete-time nonlinear system that can be expressed mathematically as

$$y(n+1) = f[y(n), ..., y(n - d_y + 1);$$
$$u(n), u(n-1), ..., u(n - d_u + 1)] \tag{3.4}$$

where $u(n) \in \mathfrak{R}$ and $y(n) \in \mathfrak{R}$ denote the model's input and output at discrete time step n, respectively, and $d_u + 1$ and $d_y + 1$, d_u and d_y, denote the input-memory and output-memory orders. The previous equation can be written as following equation in a compact shape.

$$y(n+1) = f[\mathbf{y}(n); \mathbf{u}(n)], \tag{3.5}$$

The nonlinear mapping $f[\cdot]$ is commonly unknown and can be approximated using a regular Multi-Layer Perceptron (MLP) network, for example. This gives rise to the NARX network, an influential family of dynamical models that has been shown to be computationally equivalent to Turing machines[41]. The preparation of the NARX network will take place in one of two ways:

Series-Parallel (SP) Mode; Open Loop

In this approach, the output regressor is built only by the system's actual values.

Output:

$$\hat{y}(n+1) = \hat{f}[\mathbf{y}_{sp}(n); \mathbf{u}(n)],$$
$$= \hat{f}[y(n), ..., y(n - d_y + 1); u(n), u(n-1), ..., u(n - d_u + 1)]. \tag{3.6}$$
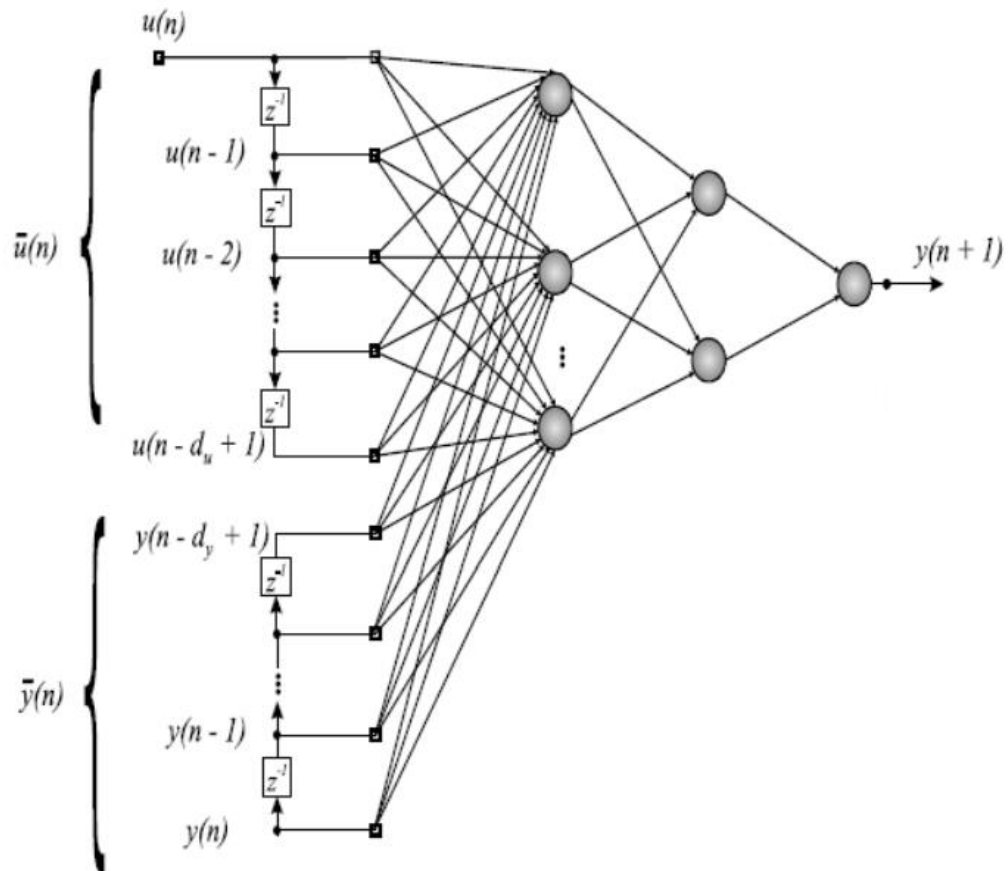
Figure 18 Architecture of the NARX network in open loop mode [41]

Parallel (P) Mode; Closed Loop

Estimated outputs are sent back and incorporated in the output's regressor in this case:

$$\hat{y}(n+1) = \hat{f}[\mathbf{y}_{sp}(n); \mathbf{u}(n)], =$$

$$\hat{f}[\hat{y}(n), ..., \hat{y}(n - d_y + 1); u(n), u(n-1), ..., u(n - d_u + 1)]. \qquad (3.7)$$

The structure of a one hidden layer NARX network in closed loop mode, which is generally used for testing or multi-step prediction, is shown in Fig. 20. As part of the conventional NARX design, the output is transmitted back to the feedforward neural network's input. The series-parallel architecture may be used to train the network in the open-loop mode, as illustrated in Fig. 19, since the network output is accessible

during training. You can only obtain one-step ahead predictions in prediction mode with an open-loop architecture, but if you want a more dynamic multi-step ahead prediction, where the first output yt+1 is fed back into the input and the process repeats for a set number of cycles, you can achieve a multi-step ahead prediction, however the accuracy will drop as the number of steps increases. All of the training, including validation and testing, is done in an open loop. We can convert the network to a closed-loop mode to conduct multistep-ahead predictions when we've finished building it in this manner. In order to improve the accuracy of multi-step forward predictions, the network's training in the open-loop mode must reduce mistakes (one-step-ahead).
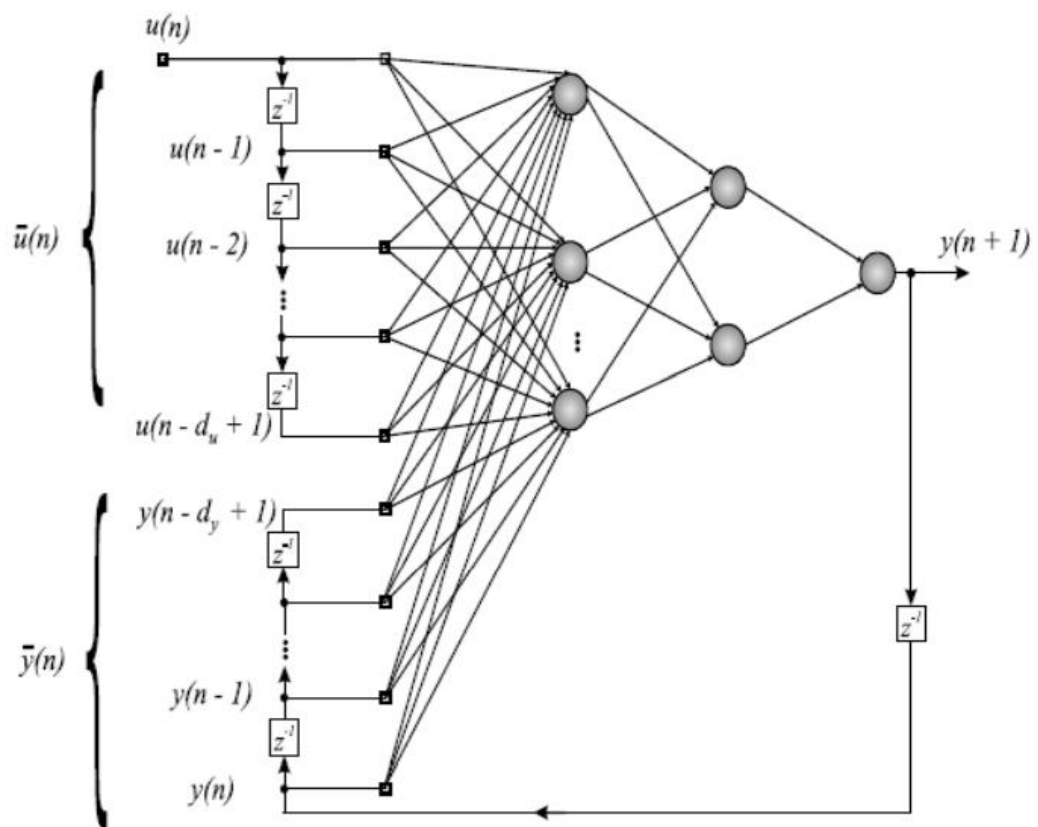
Figure 19 Architecture of the NARX network in closed loop mode [41]

3.4 proportional–integral–derivative (PID) controller

PID controller is combination of proportional, integral and derivative control actions, also called three-mode controller.

Proportional (P) Control: In this control action the output of controller is proportional to the error. A proportional controller continuously changes the manipulated variable according to error. The main disadvantage of proportional only control action is that it cannot keep the process variable on set point. The difference between controlled variable and desired set point is called steady state error or offset.

Integral (I)/Reset Control Action: The steady state error of proportional controller is removed (reset) in an integral controller. In integral control action the controller output is changed at a rate proportional to error signal. The integral control action continuously looks at the total past history of error by continuously integrating the area under the error curve.

Derivative (D) Control Action: In this control action, the controller output is function of the rate at which the error is changing. An advantage of using derivative control action is that it responds to the rate of change of actuating error and can produce a significant correction before the magnitude of actuating error becomes too large. The proportional mode considers the present state of the error, and integral control looks at its past history, while the derivative mode anticipates its future state and acts on that prediction. Derivative control anticipates process error before they have evolved and takes corrective action in advance.

Proportional-Integral-Derivative (PID) Controller: A standard PID controller is represented as:

$$m = K_p \left(e(t) + \frac{1}{T} \int_0^t e(t)dt + T_d \frac{de(t)}{dt} \right)$$

(3.8)

Transfer function of PID controller is given by

$$G(s) = K_p \left(1 + \frac{1}{T_i s} + T_d s\right) = K_p + K_i \frac{1}{s} + K_d s \; Where,$$ (3.9)

K_p = Proportional gain
K_i = Proportional gain,
K_d = Proportional gain,
T_i = Integral time constant and
T_d = Derivative time constant

3.5 Model predictive controller

Model predictive control can ensure optimal process under input/output constraints. MPC uses a dynamic model of the process system under consideration to predict and optimize the future behavior of the process over a moving horizon. The optimization block calculates a sequence of control actions at each time instant. As new process measure at each sampling instant, model parameters are updated and then, the optimization block is implemented. The facility of the MPC to handle constraints and operate with multiple inputs and outputs analytically

The MPC regularly minimizes the cost function J was calculated by

$$J = \sum_{j=N_{min}}^{N_{max}} (y_r(t+j) - \hat{y}(t+j))^2 + \rho \sum_{j=1}^{N_u} (u(t+j-1) - u(t+j-2))^2$$ (3.10)

where t is the current sampling interval, $t+1$ is a future sampling, N_{min}, N_{max} and N_u are defining the horizons over which the tracking error and the control increments are estimated. The u variable is the manipulated plant input, y_r is the reference trajectory, and $\hat{y}$ is the process model response. The ρ value is contribution that the sum of the squares of the control increments. The process constraints on the manipulated and controlled variables as follows:

$$u_{min} \leq u(t+j-1) \leq u_{max} \qquad j = 1, \dots, N_u$$

$$\Delta u_{min} \leq u(t+j-1) \leq \Delta u_{max} \qquad j = 1, \dots, N_u$$

Output variable constraint is given as:

$$y_{min} \leq \hat{y}(t+j-1) \leq y_{max} \qquad j = N_{min}, \dots, N_{max}$$

CHAPTER IV

RESEARCH METHODOLOGY

4.1 Equipment and Software

4.1.1 Laptop (ACER inter(R) core (TM) i5-8300H CPU @ 2.30GHz 8.00Gb)

4.1.2 MATLAB

4.2 PCM thermal energy storage modelling

4.2.1. Model description

The schematic diagram of the solar heat storage system is shown in Fig. 20. The TES model was designed by Shuangmao Wu et al. Based on a packed bed, a cylindrical storage tank containing spherical capsules filled with PCM (paraffin). The process is developed by adding a splitter, mixer, and domestic electric water heater to control the packed bed's temperature outlet. The splitter was split HTF into two streams to receive energy at a packed bed and then combined with another stream at the mixer. After that, the mixer's output temperature is measured to adjust the splitter faction to the control process.
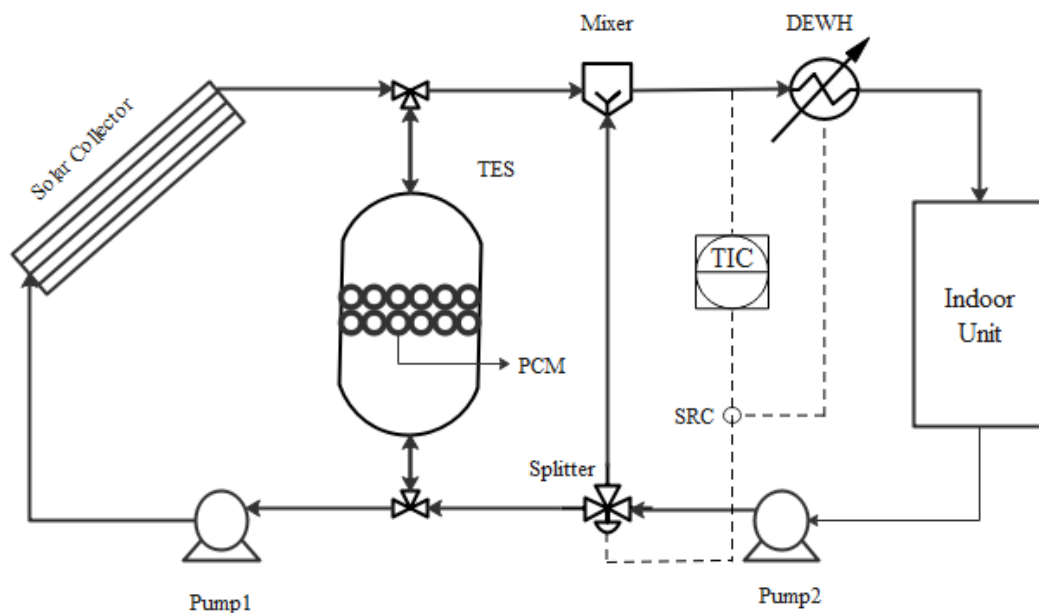
Figure 20 Solar thermal energy storage using PCM system

4.2.2 PCM thermal energy storage

The PCM for TES is a cylindrical packed bed tank modeled as a state of the discharging process. The spherical capsules in the packed bed are received energy by cool water as HTF, and the PCM in the spherical capsules change the state previously from liquid to solid. The energy equations of packed bed modeling are based on the following assumptions:

-The physical properties of the PCM and HTF are constant.

-Temperatures of PCM and HTF only differ along the axial direction.

-The natural convection in the PCM is neglected.

-The PCM does not change the temperature during phase change.

-The velocity profile is considered fully developed flow in an axial direction.

The temperature behavior of packed bed is explained through main equations which presented below.

Heat transfer fluid:

$$\rho_f \cdot c_f \cdot \varepsilon \frac{\partial T_f}{\partial t} + \rho_f \cdot c_f \cdot \varepsilon \cdot u \frac{\partial T_f}{\partial x} = k_f \cdot \varepsilon \frac{\partial^2 T_f}{\partial^2 x} + h_{eff} \cdot a_p(T_p - T_f) - h_w \cdot a_w(T_f - T_{sur}) \quad (4.1)$$

Phase change material (PCM):

Liquid phase:

$$\rho_l \cdot c_l(1 - \varepsilon) \frac{\partial T_p}{\partial t} = h_{eff} \cdot a_p(T_f - T_p) \quad (4.2)$$

Solidification process:

$$\rho_s \cdot L(1 - \varepsilon) \frac{\partial \emptyset}{\partial t} = h_{eff} \cdot a_p(T_s - T_f) \quad (4.3)$$

Solid phase:

$$\rho_s \cdot c_s(1 - \varepsilon) \frac{\partial T_p}{\partial t} = h_{eff} \cdot a_p(T_f - T_p) \quad (4.4)$$

The following are the beginning and boundary conditions for the above equations. The temperatures of HTF and PCM are above the solidification temperature at the start of the discharging procedure. So,

$$T_f(t=0)=T_i$$

$$T_p(t=0)=T_i$$

where T_i denotes the PCM and HTF starting temperatures. The fluid is expected to be at constant temperature at the packed bed's input. Therefore,

$$T_f(x=0)=T_{in}$$

HTF's inlet temperature is denoted by T_{in}. In the case of x> H, the temperature of HTF at the bed exit is assumed to be constant. Therefore,

Beek [42] created the form of correlation employed in this study for the heat transfer coefficient of spherical capsules and HTF for the situation of capsules placed in a random pattern.

$$Nu = 3.22 Re^{1/3} Pr^{1/3} + 0.117 Re^{0.8} Pr^{0.8} \qquad (4.5)$$

where Nu, Re, Pr are Nusselt number, Reynolds number and Prandtl number of HTF, respectively. Finally, the convective heat transfer coefficient was calculated.

$$h = \frac{k_f \cdot Nu}{d} \qquad (4.6)$$

The mean velocity in the bed was determined by

$$u = \frac{q_{total}}{\varepsilon \cdot A_c} \qquad (4.7)$$

where Ac and qv are the cross area of the cylindrical tank and flow rate of HTF, respectively.

Heat transmission to HTF should flow via the lid of spherical capsules during the discharging process. The thermal resistance of solidified PCM and the spherical capsule must be taken into account when calculating the heat transfer between the HTF and PCM. As a result, the effective coefficient is shown.

$$h_{eff} = \frac{h}{1 + M_c + M_s} \qquad (4.8)$$

$$M_c = \frac{R_c}{R_h} = \frac{h \cdot r_o (r_o - r_i)}{k_c \cdot r_i} \qquad (4.9)$$

$$M_s = \frac{R_s}{R_h} = \frac{h \cdot r_o^2 (r_i - r_p)}{k_s \cdot r_i \cdot r_p} \qquad (4.10)$$

where Ms and Mc are the thermal resistance of solidified PCM and capsule covers, respectively, to the thermal resistance owing to convection on the capsules' exterior surface.

4.2.3 Splitter and mixer

As the dynamic behavior of HTF temperature in PCM heat storage unit is quite fast, use of mass flow rate of HTF for control of the HTF temperature seems to be inappropriate. Furthermore, change of the mass flow rate can affect the indoor use. Therefore, a bypass is installed for temperature control. The bypass can be modelled by introducing energy balances around the splitter and mixer. As the dynamic of the splitter and mixer is very fast, steady-state models can be used and written as,

Splitter main stream into two streams:

$$q_1 = \frac{(100-P_s)q_{Totol}}{100} \tag{4.11}$$

$$q_2 = \frac{P_s \cdot q_{totol}}{100} \tag{4.12}$$

Mixer modeling:

$$T_{mix} = \frac{T_f \cdot q_1 + q_2 \cdot T_{in}}{q_{total}} \tag{4.14}$$

The parameters used in the simulation and operation of PCM thermal energy storage are listed in Table 2.

Table 2 Parameters used in PCM thermal energy storage simulation [18]

Parameter	Value
ρ_f	997 kg/m^3
C_f	4.186 kJ/ (kg K)
ρ_l	778 kg/m^3
C_l	2.38 kJ/ (kg K)
ρ_s	861 kg/m^3
C_s	1.85 kJ/ (kg K)
k_s	0.4 W/ (m K)
k_l	0.15 W/ (m K)
T_s	60 °C
L	213 kJ/kg
ε	0.45
q_{total}	10 kg/min

4.3 Design of Artificial neural network model

   4.3.1 Feed-forward neural network model

The development of ANN is to mimic the biological neural network of the human brain in problem solving processes. ANN is a black box model that connects the inputs to the outputs where the relationship between them is defined by their weights. ANN can be used for the nonlinear mapping between inputs and outputs to find model relatives or detect patterns among them.

   The three-layer feed-forward neural network is a general neural network, which consists of an input layer, hidden layer, and output layer. Each input is multiplied by weight. After that, input product is then combined with the bias in a summation form and directed to the activation function to calculate the output signals.   The procedures for the calculation can be expressed as,

$$sum = b + \sum_{i=1}^{n} x_i \cdot w_i \tag{4.15}$$

Where w_i and b are the weight and the bias coefficient of the neuron. x_i refers to the input of each layer. The net output signal of each neuron is transferred to the activation function. Sigmoid tangent function is shown in Eq. (9).

$$n = f(sum) = \frac{e^{sum} - e^{-sum}}{e^{sum} + e^{-sum}} \tag{4.16}$$

   4.3.2 Proposed feed-forward neural network model for the prediction of the
     HTF outlet temperature

The proposed ANN model is based on a multi-layer perceptron (MLP) consisting of four inputs (time, HTF inlet temperature, HTF mass flow rate, and initial PCM temperature) and one output (HTF outlet temperature) as shown in figure 21. The data for ANN training was generated by performing the simulation of the PCM heat storage unit under various input conditions, 25-35 ° C for HTF inlet temperatures, 1-10 kg /min for HTF

mass flow rates, and 70-90 °C for initial PCM temperatures and then observing changes of HTF outlet temperatures under time span 0-12,500 seconds. Random white noises ± 2% are added into the data. The data are divided into three sets, 70% for training, 15% for validation, and 15% for testing.
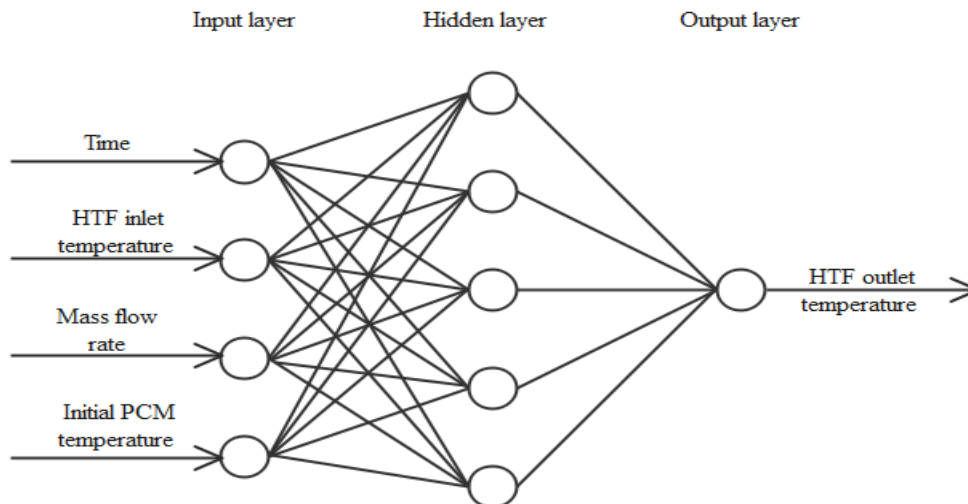
Figure 21 The structure of the proposed feed-forward neural network model.

　　4.3.3 Design nonlinear autoregressive network with exogenous inputs (NARX) In terms of the number of hidden layers in the model, the number of neurons in each layer, the transfer function used in each layer, the training algorithm, and the number of delays in the NARX model, several configurations were tested to determine the optimal NARX recurrent neural network architecture. The best correlation coefficient (R) and the smallest root mean square error should be found in the best model (RMSE). The difference between the predicted and measured data is measured using RMSE. The R value denotes the relationship between the predicted output and the desired outcome. The R value is in the [-1, 1] range. If R = 1, the output and the targets have a very strong positive relationship. The feed forward neural network was used in this study. There are two layers in this network: a single hidden layer and an output layer. The tangent sigmoid function in the hidden layer and the linear function in the output layer are the transfer functions used in the network. In addition, the delays of each

input must be identified in relation to the number of neurons in the hidden layer in order to design the network architecture. In addition, the Levenberg-Marquardt (LM) training algorithm was used in the recurrent neural network's training phase.

4.4 Design controller of HTF temperature

For application of PCM heat storage unit to domestic water heating, the HTF temperature need to be satisfied. A bypass is installed and the split fraction is used as manipulated variable for the temperature control. Furthermore, for simplicity PI control is used.

4.4.1 PI controller with optimization method

As the model of PCM heat storage unit is quite complex, no simple transfer function is available for tuning of PI controller. Although online trial-and-error tuning method such as Ziegler-Nichols method requires no knowledge of the model, it is quite tedious. In this work, an optimization approach was used for the controller tuning. The proposed ANN model was used for the prediction of control performance, i.e., integral square error (ISE), under various sets of proportional gain and integral time constant. The tuning set that minimizes the ISE is chosen.
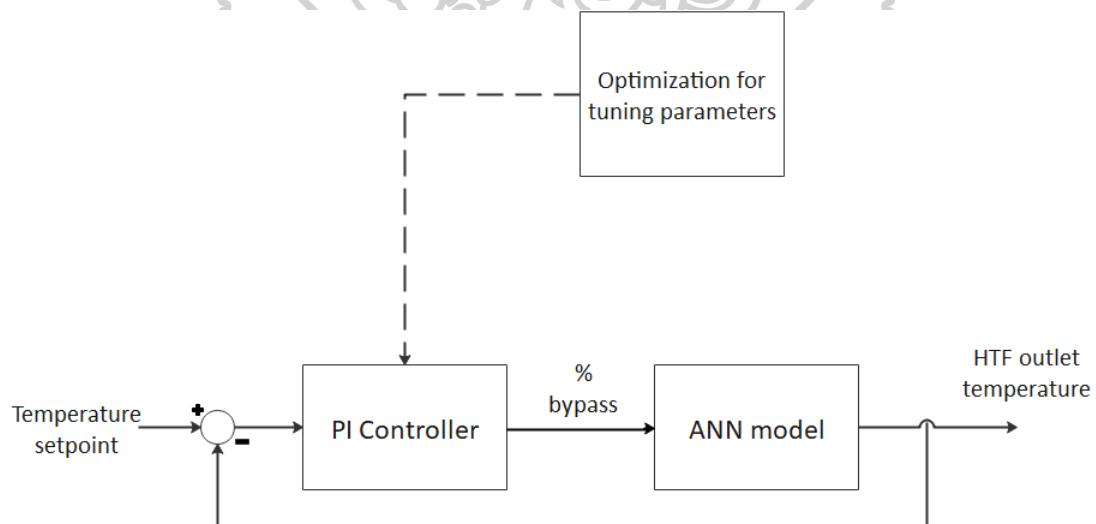
Figure 22 The structure of PI controller using optimization method with ANN model

4.4.2 Neural network-based model predictive controller (NNMPC)

Model predictive control begins with the training of a neural network to reflect the plant's forward dynamics. The neural network training signal is the prediction error between the plant output and the neural network output. The neural network plant model predicts future plant output values based on prior inputs and plant outputs. Using data obtained from the plant's operation, this network may be taught offline in the PCM thermal energy storage model. The receding horizon approach is used in the model predictive control approach. The plant reaction is predicted by a neural network model over a certain time horizon. A numerical optimization software uses the predictions to find the control signal that minimizes the following performance criteria over the chosen time horizon. For more information about MPC, go here. It was discussed before in this section.

$$J = \sum_{j=N_{min}}^{N_{max}} (y_r(t+j) - \hat{y}(t+j))^2 + \rho \sum_{j=1}^{N_u} (u(t+j-1) - u(t+j-2))^2 \qquad (4.17)$$
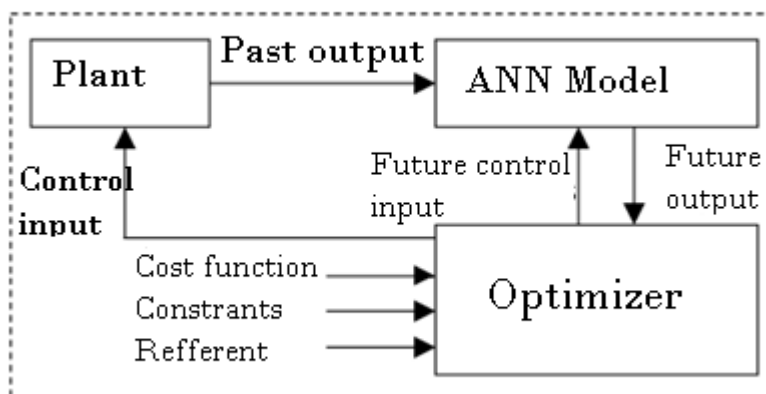
Figure 23 Neural network-based model predictive control loop

CHAPTER V

RESULT AND DISCUSSION

5.1 Open-loop simulation of PCM system

To understand the behavior of PCM heat storage unit, an open-loop simulation was firstly performed. The mass flow rate and inlet temperature of HTF used are 10 kg/min and 30 $C°$, respectively. Initial temperatures of HTF and PCM are assumed as 70 $C°$. As shown in figure 24, there are three stages during discharging process including liquid cooling where the temperature of PCM gradually decreases, solidification (liquid-solid phase change) where the temperature of PCM remains constant at the solidification temperature, and solid cooling where the temperature of PCM decreases rapidly to the inlet temperature of HTF. For the temperature of HTF, it follows the temperature of PCM very closely, except during the stage of solid cooling as the heat transfer decreases due to less temperature difference between PCM and HTF.

Figure 24 H

Figure 25 shows the effects of HTF mass flow rate (ranging from 10 to 20 kg/min) on HTF temperature outlet. As the HTF mass flow rate increases, the operating time for liquid cooling and solidification phase reduces. Due to this, the period that is allocated to the use of solar energy storage is used quicker.
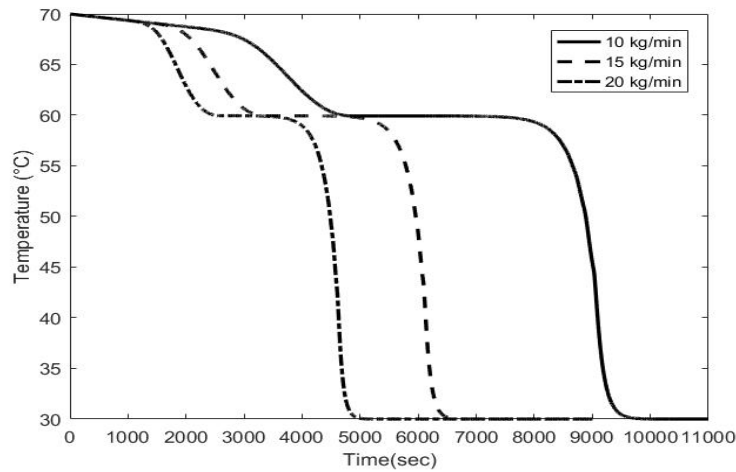
Figure 25 HTF temperature outlet evolution for different mass flow rate

5.2 ANN modeling of PCM system

5.2.1 Feed-forward neural network model

In developing ANN model, the number of hidden layers and the number of hidden neurons need to be determined. In this work, the numbe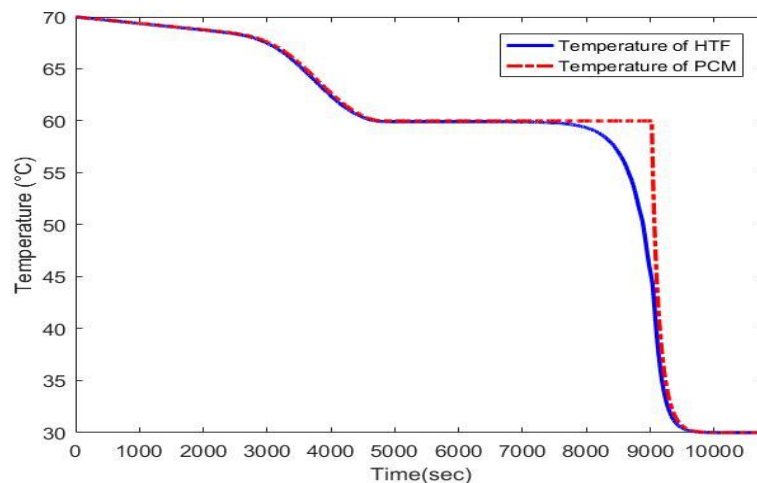r of hidden layers chosen is one for simplicity and as it can represent most of the data quite well. In finding the number of hidden neurons, the ANN with various number of hidden neurons is trained and the smallest one that provides acceptable statistical accuracy indices, i.e., mean square error (MSE) and regression coefficient (R^2) is chosen.

As shown in Table 3, the performance of ANN model continuously increases as the number of hidden neurons increases until up to sixteen. Thus, the sixteen-hidden neuron is an optimal number of hidden neurons and the selected ANN structure is 4-16-1(input-hidden-output). For training algorithms, Table 4 showed that Levenberg-Marquardt was the best as it provided the least MSE.

In testing the performance of the proposed ANN model, simulation results generated from the PCM heat storage model with white noise ± 2% and the ANN model are compared as shown in figure 26. The conditions used in this simulation are random 30-40 C^o for the HTF inlet temperature, 10 kg/min for HTF mass flow rate, and 70 C^o for initial PCM temperature. Good agreement in the results can be found.

Table 3 Determination of the best topology of the ANN feed-forward model with different number of hidden neurons

Number of hidden	Train		Test	
neurons	MSE	R^2	MSE	R^2
1	1.92×10^{-2}	0.833033	1.89×10^{-2}	0.830946
2	1.52×10^{-2}	0.871209	1.52×10^{-2}	0.870539
3	5.15×10^{-3}	0.958062	5.05×10^{-3}	0.958225
4	4.16×10^{-3}	0.966372	4.28×10^{-3}	0.965918
5	3.94×10^{-3}	0.968395	3.85×10^{-3}	0.967900
6	3.57×10^{-3}	0.971103	3.65×10^{-3}	0.970540
7	3.06×10^{-3}	0.975477	3.07×10^{-3}	0.975142
8	2.87×10^{-3}	0.976941	2.88×10^{-3}	0.975932
9	2.73×10^{-3}	0.977955	2.79×10^{-5}	0.978040
10	2.60×10^{-3}	0.978864	2.67×10^{-3}	0.977964
11	2.43×10^{-3}	0.980281	2.48×10^{-3}	0.980235
12	2.28×10^{-3}	0.981598	2.33×10^{-5}	0.980799
13	2.25×10^{-3}	0.981824	$2.32 \times 10^{-}$	0.981499
14	2.19×10^{-3}	0.982331	2.21×10^{-3}	0.981770
15	2.15×10^{-3}	0.982578	2.15×10^{-3}	0.982757
16	2.14×10^{-3}	0.982824	2.14×10^{-3}	0.982814
17	2.16×10^{-3}	0.982696	2.17×10^{-6}	0.982596
18	2.17×10^{-3}	0.982664	2.19×10^{-3}	0.982410
19	2.17×10^{-3}	0.982573	2.19×10^{-3}	0.982275
20	2.19×10^{-3}	0.982430	2.20×10^{-3}	0.982074

Note: The best-obtained results among 30 various are trained networks per each hidden neuron.

Table 4 Determination training algorithm of the ANN feed-forward model

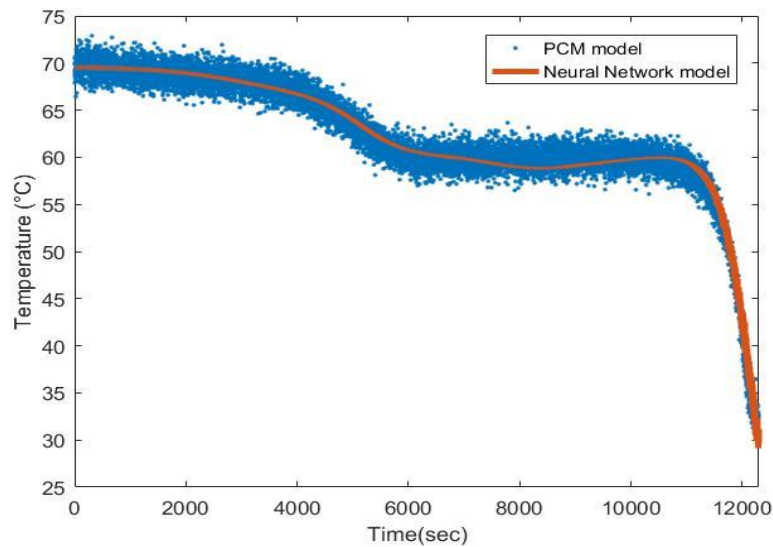| Training algorithm	MSE	R^2	Processing time (s/epochs)
Bayesian regulation backpropagation	2.25×10^{-3}	0.981844	0.0253
Levenberg-Marquardt backpropagation	2.14×10^{-3}	0.982824	0.0238
Scaled conjugate gradient backpropagation	2.37×10^{-3}	0.980517	0.0182

Figure 26 The prediction of HTF outlet temperature using the proposed ANN model

5.2.2 Nonlinear autoregressive network with exogenous inputs (NARX)

In NARX NN model, feedforward neural network was used to predict the parameters of the NARX model of the PCM. The NARX model has two inputs (HTF inlet temperature, % of bypass) and one output (HTF outlet temperature). As demonstrated in Table 5, the performance of the ANN model improves linearly with the number of hidden neurons until it reaches eleven. Thus, the optimum number of hidden neurons was eleven. Following that, we evaluate several training methods to determine the best one. These algorithms include Levenberg–Marquardt, Bayesian regulation, and Scaled conjugate gradient backpropagation. Then, by varying model delay from 2 to 18, we can get the NARX model's optimum delay value. Table 6 showed the Levenberg–Marquardt method was the best while Table 7 showed 12 delays was the optimum number of delays. NARX model was firstly developed as an open-loop version where the current output was function of past outputs and past inputs. After that it was transform to a closed-loop version where the current output was function of past inputs only. Both open-loop and closed-loop NARX forms were tested with a set of new generated data and the results showed the good prediction could be expected.

Table 5 Determination of the best topology of the NARX model with different number of hidden neurons

Number of hidden neurons	Train		Test	
	MSE	R^2	MSE	R^2
1	1.45×10^{-2}	0.999523	1.50×10^{-2}	0.999510
2	1.41×10^{-2}	0.999538	1.42×10^{-2}	0.999535
3	1.42×10^{-2}	0.999533	1.34×10^{-2}	0.999570
4	1.41×10^{-2}	0.999540	1.38×10^{-2}	0.999532
5	1.34×10^{-2}	0.999558	1.34×10^{-2}	0.999564
6	1.34×10^{-2}	0.999554	1.35×10^{-2}	0.999562
7	1.34×10^{-2}	0.999558	1.33×10^{-2}	0.999565
8	1.35×10^{-2}	0.999559	1.31×10^{-2}	0.999579
9	1.33×10^{-2}	0.999561	1.31×10^{-2}	0.999577
10	1.33×10^{-2}	0.999565	1.35×10^{-2}	0.999560
11	1.31×10^{-2}	0.999572	1.31×10^{-2}	0.999579
12	1.31×10^{-2}	0.999570	1.32×10^{-2}	0.999566
13	1.32×10^{-2}	0.999567	1.34×10^{-2}	0.999531
14	1.32×10^{-2}	0.999563	1.33×10^{-2}	0.999561
15	1.30×10^{-2}	0.999573	1.33×10^{-2}	0.999557
16	1.31×10^{-2}	0.999569	1.34×10^{-2}	0.999561
17	1.33×10^{-2}	0.999564	1.33×10^{-2}	0.999561
18	1.33×10^{-2}	0.999559	1.34×10^{-2}	0.999549
19	1.32×10^{-2}	0.999565	1.35×10^{-2}	0.999545
20	1.32×10^{-2}	0.999566	1.33×10^{-2}	0.999572

Note: The best-obtained results among 30 various are trained networks per each hidden neuron.

Table 6 Determination of the best delay of the NARX model with different number of delays.

Number of delays	MSE	R^2	Processing time (s/epochs)
2	0. 01314	0.999579	0.024
4	0.01284	0.999589	0.048
6	0.01124	0.999624	0.083
8	0.01142	0.999618	0.157
10	0.01021	0.999639	0.193
12	0.01007	0.999652	0.214
14	0.01050	0.999650	0.291
16	0.01082	0.999646	0.333
18	0.01076	0.0999637	0.370

Table 7 Determination of the best training algorithm of the NARX model

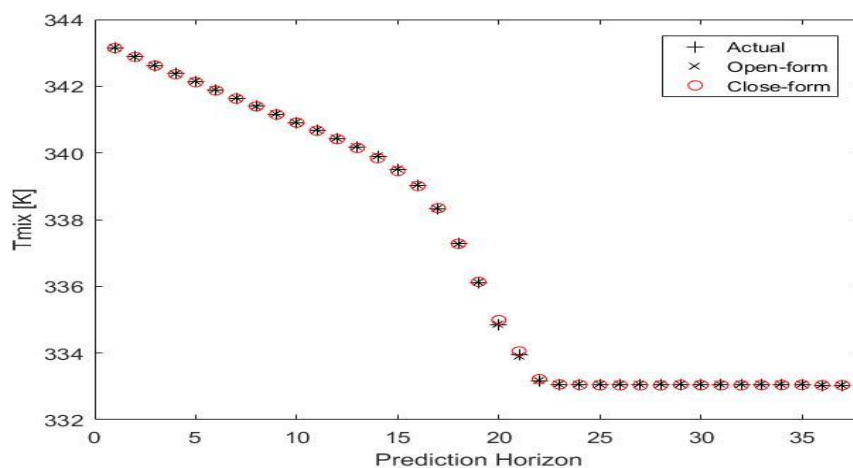| Training algorithm	MSE	R^2	Processing time (s/epochs)
Bayesian regulation backpropagation	0.01164	0.999622	0.241
Levenberg-Marquardt backpropagation	0.01007	0.999652	0.214
Scaled conjugate gradient backpropagation	0.01191	0.999640	0.0187

Figure 27 The comparison between actual and prediction value of NARX model

5.3 Application PCM in water heating

5.3.1 Neural-network-based PI controller

As there was no steady-state of the system, a normal tuning method of PI controller could not be applied. Hence, an optimization approach was used. By varying a set of tuning parameters of PI, the set of parameters providing the best ISE was chosen.

Under a given set of Kc and Ti in the ranges of -5 to 0 (negative effect required) and 0 to 5, respectively, the proposed ANN model combing with the mixer model was used to predict the closed-loop response of HTF temperature. Figure 28 shows the plot between integral square error (ISE) and PI parameters. Less ISE can be obtained in the dark blue region. As no significant difference of ISE in this region, Kc = 1 and Ti = 1 were chosen as our choice.

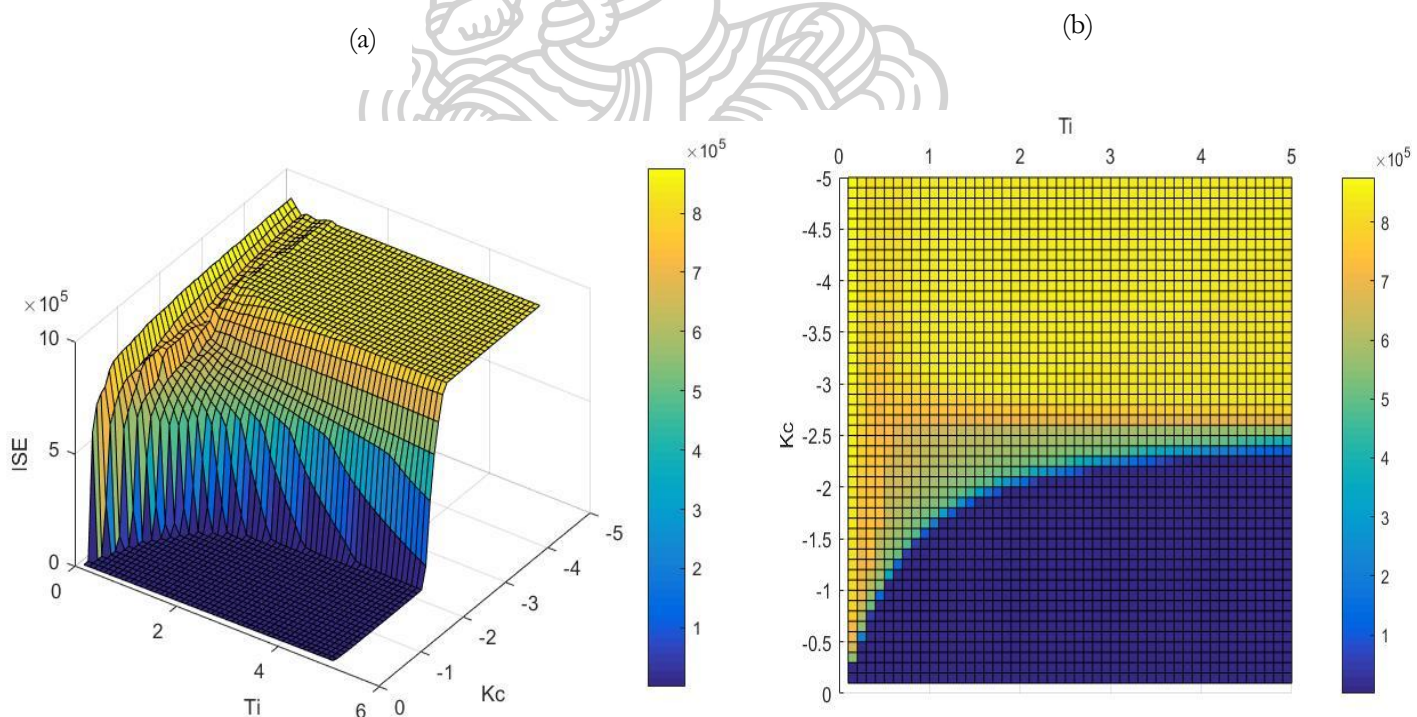(a)   (b)

Figure 28 Effect PI parameters to ISE predicted from the proposed ANN model in (a) 3D plot and (b) contour plot

The PI controller tuned in the previous section was used in control test of the water heating system with PCM as heat storage unit for both setpoint tracking and disturbance rejection as shown in figures 29 and 30. In figure 29, +5 $C°$ step change of the setpoint was made while in figure 30, +5 $C°$ step change of the HTF inlet temperature was introduced. The results showed that with a bypass installed to the system, the HTF temperature was controlled very well as the fast response could be expected.

Figure 31 showed the response of the HTF temperature under a long period operation. Note that after a long run, the HTF temperature could not be kept at the setpoint. This was because the heat storage in the PCM was over.
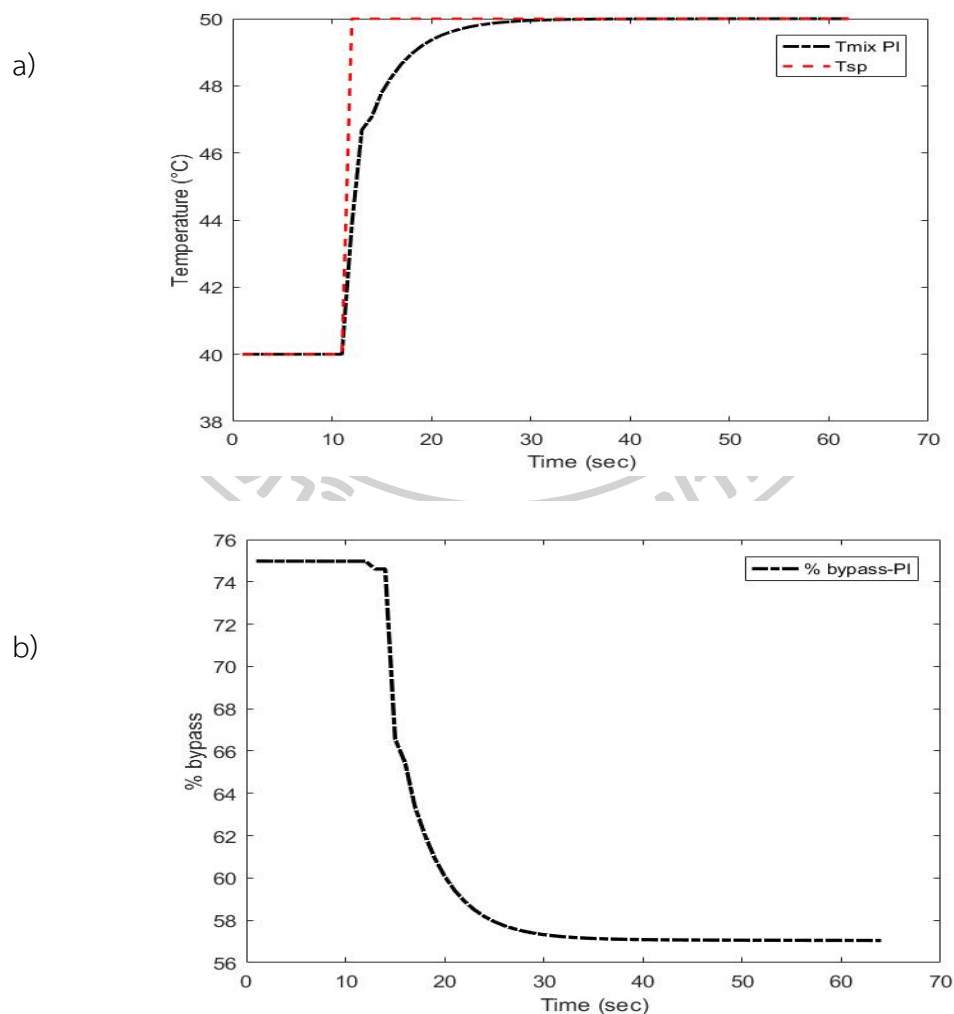
a)

b)

Figure 29 PI controller plot of (a) HTF temperature and (b) percent of bypass under closed-loop simulation of setpoint tracking case.
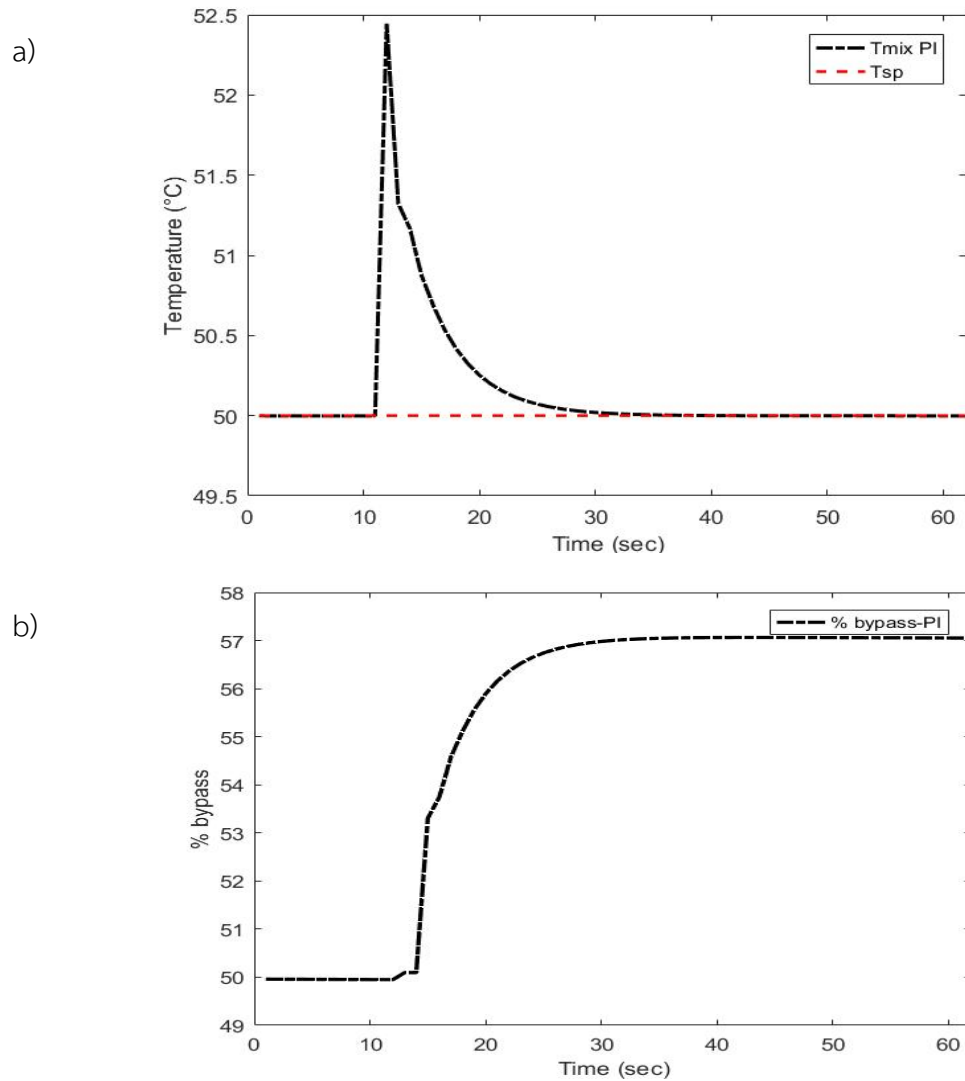
a)

b)

Figure 30 PI controller plot of (a) HTF temperature and (b) percent of bypass under closed-loop simulation of disturbance rejection case
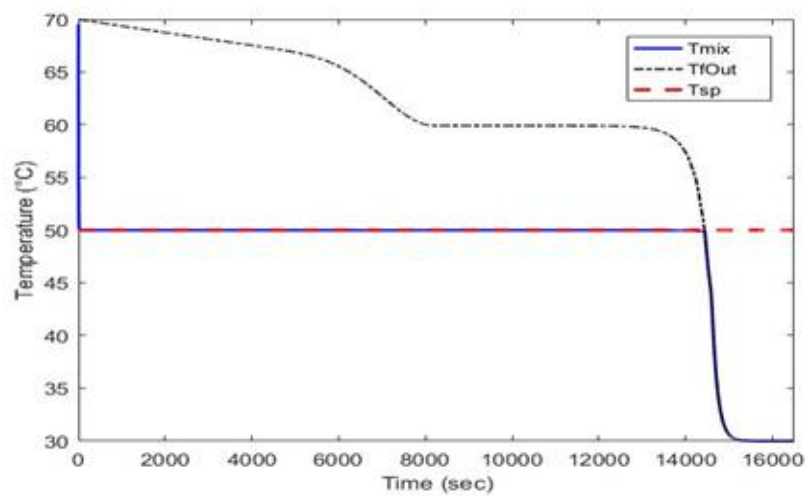

Figure 31 PI controller response of HTF temperature operated under a long period

5.3.2 MPC controller of water heating system

In development of MPC, as the model of PCM was quite tedious and complex, hence NARX neural network was used for model prediction in MPC. This would be called neural network MPC (NNMPC) in this work.

In tuning of the MPC, the number of control horizon, prediction horizon, and weight coefficients of the input need to be determined. In variation of these parameters, as the control horizon (Nu) = 1 could provide satisfied performance, hence, the number of prediction horizon (Np) was also set to 1 as it could not be more than Nu. The Np = 1 was equivalent to Nmin = Nmax = 1 in the section 4.4.2. The weight coefficient of the input in the cost function was chosen as 0.6.

The NNMPC controller tuned in the previous section was used in control test of the water heating system with the PCM as heat storage unit for both setpoint tracking and disturbance rejection as shown in figures 32 and 33. In figure 32, +10 $C°$ step change of the setpoint was made while in figure 33, +5 $C°$ step change of the HTF inlet temperature was introduced. The results of NNMPC showed that with a bypass installed to the system, the HTF temperature was controlled very well as the fast response could expected. Finally, the NNMPC and the PI controller were evaluated in terms of set point tracking performance. Figure 34 shows that, even with little oscillation, NNMPC was able to move the system to the new setpoint more rapidly.
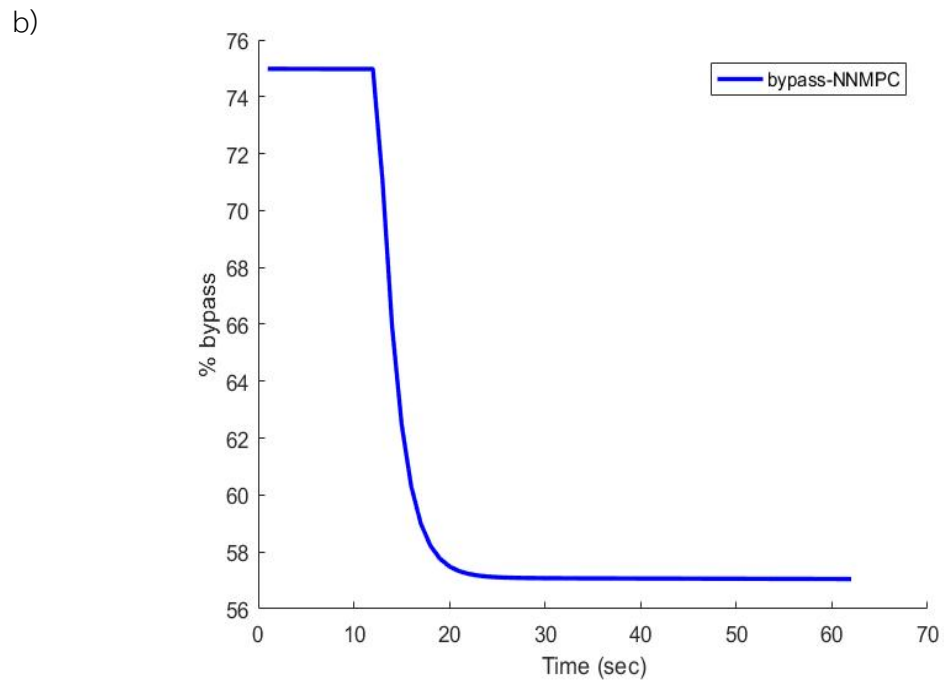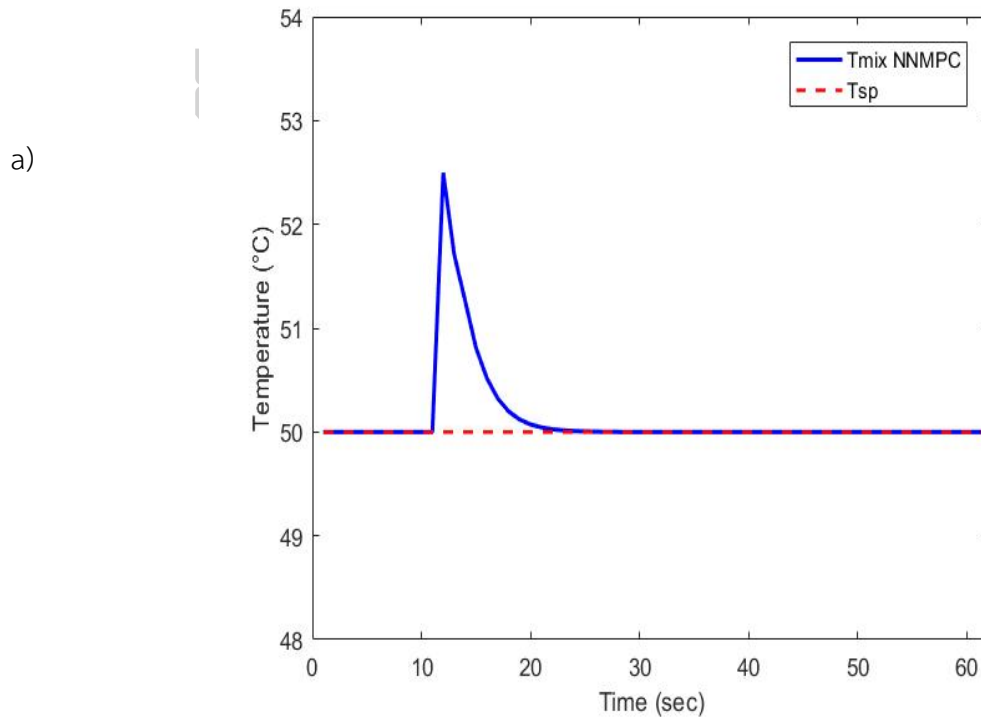
a)

b)
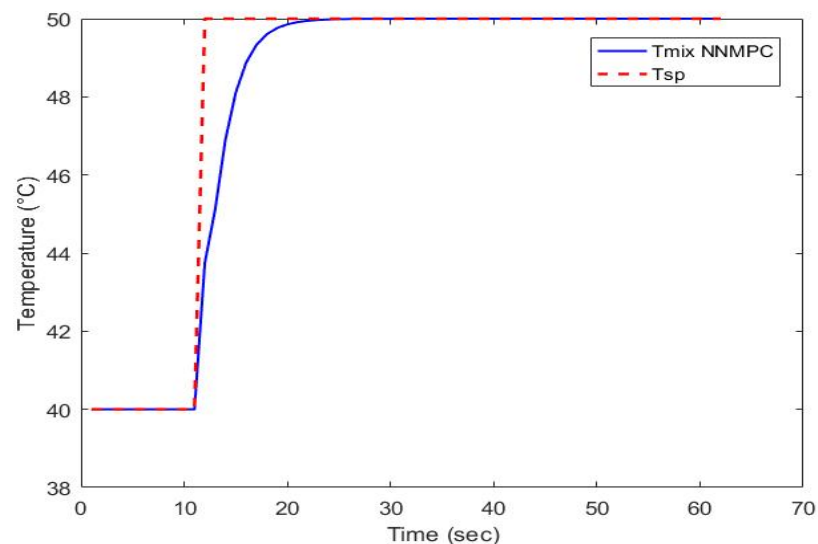
Figure 32 NNMPC controller plot of (a) HTF temperature and (b) percent of bypass under closed-loop simulation of setpoint tracking case.
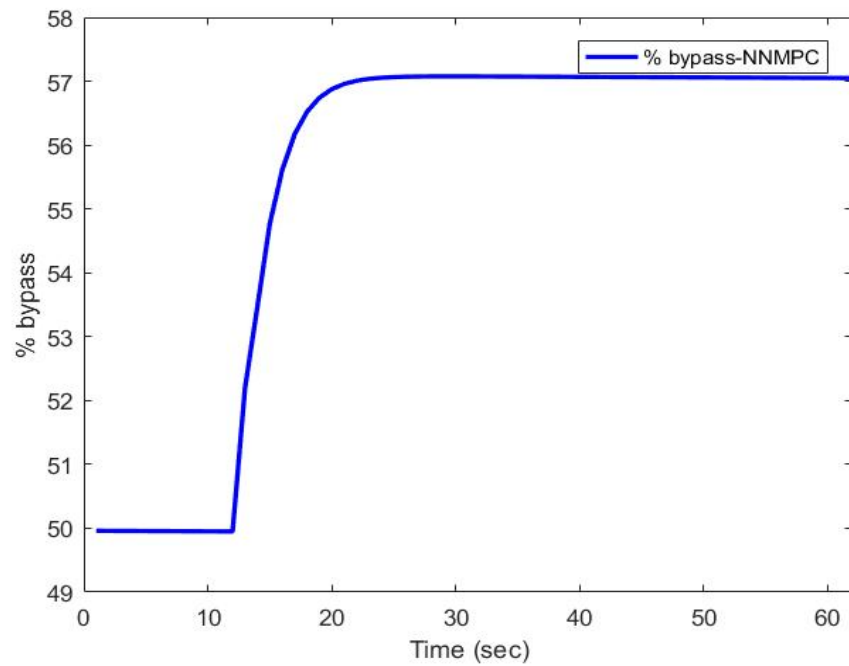
a)

b)

Figure 33 NNMPC controller plot of (a) HTF temperature and (b) percent of bypass under closed-loop simulation of disturbance rejection case
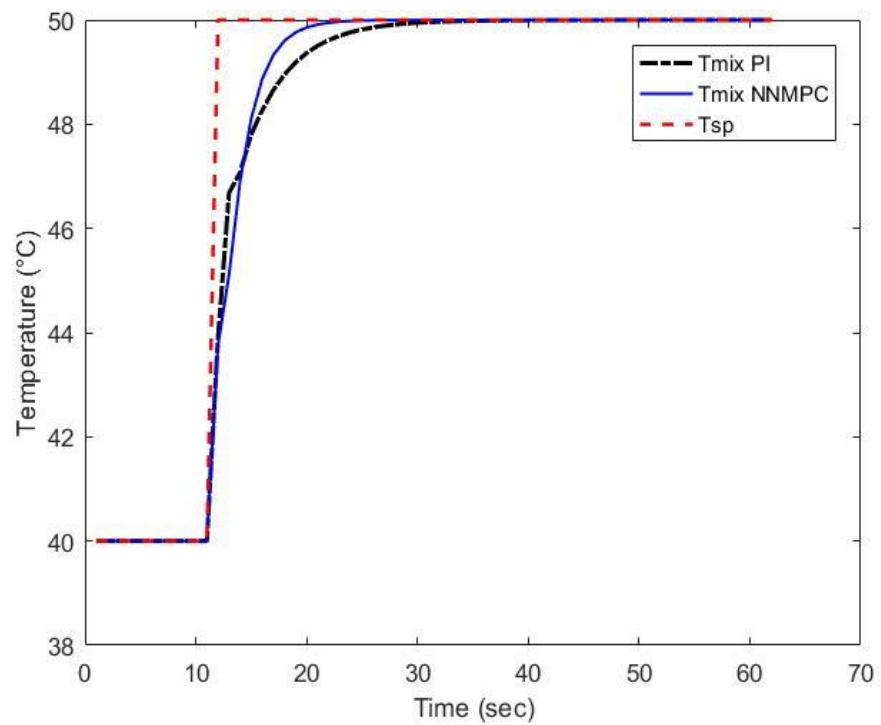

*Figure 34 The comparison step responds between NNMPC and PI controller.*

CHAPTER VI

CONCLUSION AND RECOMMENDATIONS

6.1 Conclusions

PCMs are a potential option for thermal energy storage. Due to the nature of latent heat storage, it is capable of storing a significant quantity of heat with less temperature change than sensible heat storage. PCM may be used in a variety of ways as a solar heat storage unit. Solar water heating utilizes water as a heat transfer fluid (HTF) to absorb energy from the sun throughout the day. Excess energy will be stored or charged to PCM and then released or discharged for usage during the night. Temperature management is often not required during the PCM charging procedure. However, the PCM discharge method requires a goal temperature of hot water for interior usage. The goals of this study are to create an artificial neural network model for the PCM discharging process and to design a temperature control system for the hot water discharged by the PCM for indoor usage. Two methods were suggested for the creation of the ANN model. The initial method tried to directly anticipate PCM behavior using a feedforward neural network. Time, HTF inlet temperature, mass flowrate, and starting PCM temperature are all inputs to the ANN. The second method utilized a feedforward neural network to forecast the parameters of a nonlinear autoregressive exogenous (NARX) model that was used to anticipate PCM behavior. A bypass was also built and utilized as a manipulated variable in the design of the temperature regulation of hot water in the PCM discharge process. We developed PI and MPC controllers. While both controllers were capable of controlling the temperature, MPC demonstrated superior control capability.

6.2 Recommendations

1. A more analysis for the comparison between the two proposed ANN models should be performed as in this work, the data sets for training for each model were different.

2. A data set for the training of the ANN model 1 (for direct prediction the PCM behavior) was quite big as the number of data depended strongly on the time step generated from ODE solvers. Some methods to reduce the unnecessary data might be useful.

3. As the closed-loop response of the system was very fast and an offset was found under operation using NNMPC. This caused more ISE value for the more number of prediction horizon (N_p) resulting in the best N_p = 1. In general, if there was no offset, the more N_p should provide better control performance.
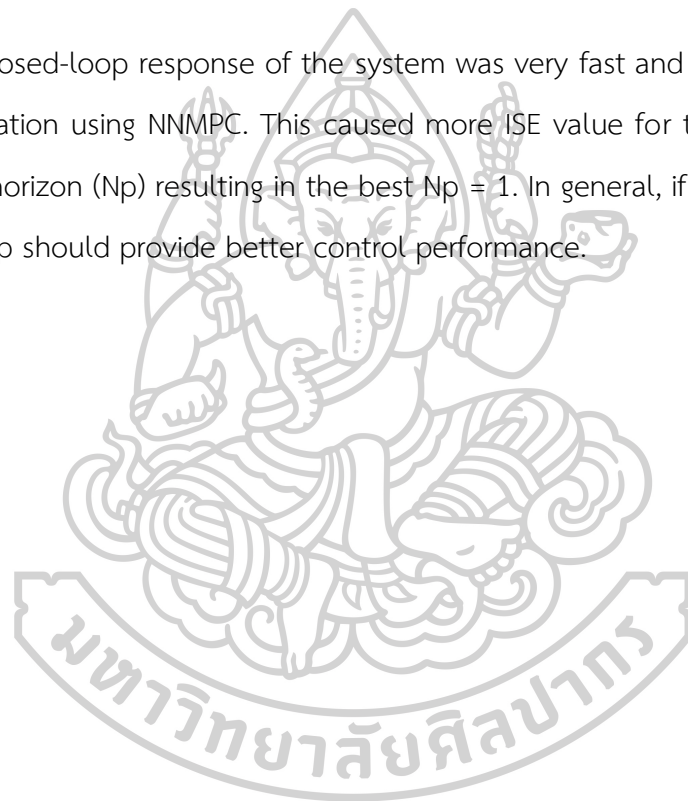
REFERENCES

1. Yagi, J. and T. Akiyama, *Storage of thermal energy for effective use of waste heat from industries.* Journal of Materials Processing Technology, 1995. **48**(1): p. 793-804.

2. Pitié, F., et al., *Circulating fluidized bed heat recovery/storage and its potential to use coated phase-change-material (PCM) particles.* Applied Energy, 2013. **109**: p. 505-513.

3. Shukla, A., D. Buddhi, and R.L. Sawhney, *Solar water heaters with phase change material thermal energy storage medium: A review.* Renewable and Sustainable Energy Reviews, 2009. **13**(8): p. 2119-2125.

4. Ait Hammou, Z. and M. Lacroix, *A hybrid thermal energy storage system for managing simultaneously solar and electric energy.* Energy Conversion and Management, 2006. **47**(3): p. 273-288.

5. Wu, W., et al., *A novel composite PCM for seasonal thermal energy storage of solar water heating system.* Renewable Energy, 2020. **161**: p. 457-469.

6. Mahfuz, M.H., et al., *Performance investigation of thermal energy storage system with Phase Change Material (PCM) for solar water heating application.* International Communications in Heat and Mass Transfer, 2014. **57**: p. 132-139.

7. Tyagi, V.V. and D. Buddhi, *PCM thermal storage in buildings: A state of art.* Renewable and Sustainable Energy Reviews, 2007. **11**(6): p. 1146-1166.

8. Zhang, Y., et al., *Application of latent heat thermal energy storage in buildings: State-of-the-art and outlook.* Building and Environment, 2007. **42**(6): p. 2197-2209.

9. He, Z., et al., *Cyclic characteristics of water thermocline storage tank with encapsulated PCM packed bed.* International Journal of Heat and Mass Transfer, 2019. **139**: p. 1077-1086.

10. Mao, Q. and Y. Zhang, *Thermal energy storage performance of a three-PCM cascade tank in a high-temperature packed bed system.* Renewable Energy, 2020. **152**: p. 110-119.

11. Loem, S., et al., *Thermal characteristics on melting/solidification of low temperature PCM balls packed bed with air charging/discharging.* Case Studies in Thermal Engineering, 2019. **14**: p. 100431.

12. Liao, Z., et al., *A novel effective thermal conductivity correlation of the PCM melting in spherical PCM encapsulation for the packed bed TES system.* Applied Thermal Engineering, 2018. **135**: p. 116-122.

13. Adine, H.A. and H. El Qarnia, *Numerical analysis of the thermal behaviour of a shell-and-tube heat storage unit using phase change materials.* Applied Mathematical Modelling, 2009. **33**(4): p. 2132-2144.

14. Kalogirou, S.A., *Artificial neural networks in renewable energy systems applications: a review.* Renewable and Sustainable Energy Reviews, 2001. **5**(4): p. 373-401.

15. Kalogirou, S.A., *Applications of artificial neural networks in energy systems.* Energy Conversion and Management, 1999. **40**(10): p. 1073-1087.

16. Rathod, M.K. and J. Banerjee, *Thermal stability of phase change materials used in latent heat energy storage systems: A review.* Renewable and Sustainable Energy Reviews, 2013. **18**: p. 246-258.

17. Abhat, A., *Low temperature latent heat thermal energy storage: Heat storage materials.* Solar Energy, 1983. **30**(4): p. 313-332.

18. Yang, L., X. Zhang, and G. Xu, *Thermal performance of a solar storage packed bed using spherical capsules filled with PCM having different melting points.* Energy and Buildings, 2014. **68**: p. 639-646.

19. Deng, J., et al., *Thermal performance assessment and improvement of a solar domestic hot water tank with PCM in the mantle.* Energy and Buildings, 2018. **172**: p. 10-21.

20. *Solar heat storage: Latent heat materials—Vol. I: Background and scientific principles: George A. Lane, Ph.D. (Editor). CRC Press, Boca Raton, Florida, 1983, 238 pp: Cost $76.00.* Solar Energy, 1984. **33**(5): p. 476.

21. Zalba, B., et al., *Review on thermal energy storage with phase change: materials, heat transfer analysis and applications.* Applied Thermal Engineering, 2003. **23**(3): p. 251-283.

22. Sharif, M.K.A., et al., *Review of the application of phase change material for heating and domestic hot water systems.* Renewable and Sustainable Energy Reviews, 2015. **42**: p. 557-568.

23. Peng, H., et al., *Modeling on heat storage performance of compressed air in a packed bed system.* Applied Energy, 2015. **160**: p. 1-9.

24. Cho, K. and S.H. Choi, *Thermal characteristics of paraffin in a spherical capsule during freezing and melting processes.* International Journal of Heat and Mass Transfer, 2000. **43**(17): p. 3183-3196.

25. Nallusamy, N., S. Sampath, and R. Velraj, *Study on performance of a packed bed latent heat thermal energy storage unit integrated with solar water heating system.* Journal of Zhejiang University-SCIENCE A, 2006. **7**(8): p. 1422-1430.

26. Oró, E., et al., *Stratification analysis in packed bed thermal energy storage systems.* Applied Energy, 2013. **109**: p. 476-487.

27. Peng, H., H. Dong, and X. Ling, *Thermal investigation of PCM-based high temperature thermal energy storage in packed bed.* Energy Conversion and Management, 2014. **81**: p. 420-427.

28. Nagano, K., et al., *Thermal characteristics of a direct heat exchange system between granules with phase change material and air.* Applied Thermal Engineering, 2004. **24**(14): p. 2131-2144.

29. Wu, S., G. Fang, and X. Liu, *Dynamic discharging characteristics simulation on solar heat storage system with spherical capsules using paraffin as heat storage material.* Renewable Energy, 2011. **36**(4): p. 1190-1195.

30. Felix Regin, A., S.C. Solanki, and J.S. Saini, *An analysis of a packed bed latent heat thermal energy storage system using PCM capsules: Numerical investigation.* Renewable Energy, 2009. **34**(7): p. 1765-1773.

31. Al Abdallat, Y., et al., *Development of Neural Networks for Enhancement of thermal energy storage using phase change material.* International Journal of Thermal and Environmental Engineering (IJTEE), 2013. **5**: p. 167–173.

32. Ermis, K., A. Erek, and I. Dincer, *Heat transfer analysis of phase change process in a finned-tube thermal energy storage system using artificial neural network.* International Journal of Heat and Mass Transfer, 2007. **50**(15): p. 3163-3175.

33. Delcroix, B., M. Kummert, and A. Daoud, *MODELING PHASE-CHANGE MATERIALS HEAT CAPACITY USING ARTIFICIAL NEURAL NETWORKS.* 2018. **49**(7): p. 617-631.

34. Baby, R. and C. Balaji, *A Neural Network-Based Optimization Of Thermal Performance Of Phase Change Material-Based Finned Heat Sinks—An Experimental Study.* Experimental Heat Transfer, 2013. **26**(5): p. 431-452.

35. Draeger, A., S. Engell, and H. Ranke, *Model predictive control using neural networks.* IEEE Control Systems Magazine, 1995. **15**(5): p. 61-66.

36. Lazar, M. and O. Pastravanu, *A neural predictive controller for non-linear systems.* Mathematics and Computers in Simulation, 2002. **60**(3): p. 315-324.

37. Yu, B. and J. Zhu. *Neural Network Model Predictive Control with Genetic Algorithm Optimization and Its Application to Turbofan Engine Starting.* in *2010 Second International Conference on Intelligent Human-Machine Systems and Cybernetics*. 2010.

38. Hang, X., T. Hao, and L. Yu-He. *Time series prediction based on NARX neural networks: An advanced approach.* in *2009 International Conference on Machine Learning and Cybernetics*. 2009.

39. Gavin, H. *The Levenberg-Marquardt method for nonlinear least squares curve-fitting problems c ©.* 2013.

40. Gouravaraju, S., et al., *A Bayesian regularization-backpropagation neural network model for peeling computations.* 2020.

41. Menezes, J.M.P. and G.A. Barreto, *Long-term time series prediction with the NARX network: An empirical evaluation.* Neurocomputing, 2008. **71**(16): p. 3335-3343.

42. Beek, J., *Design of Packed Catalytic Reactors*, in *Advances in Chemical Engineering*, T.B. Drew, J.W. Hoopes, and T. Vermeulen, Editors. 1962, Academic Press. p. 203-271.

VITA

NAME	Mr.Chanachai Phumcha-em
DATE OF BIRTH	18 January 1996
PLACE OF BIRTH	Nakhon Pathom
INSTITUTIONS ATTENDED	Silpakorn University
HOME ADDRESS	151 Malaiman, Lumpaya, Mueng, Nakhon Pathom, 73000